EDGEWOOD
CHEMICAL BIOLOGICAL CENTER
U.S. ARMY RESEARCH, DEVELOPMENT AND ENGINEERING COMMAND

ECBC-TR-596

EVAPORATION OF HD DROPLETS FROM NONPOROUS, INERT SURFACES IN TGA MICROBALANCE WIND TUNNELS

Seok H. Hong
Kenneth B. Sumpter

RESEARCH AND TECHNOLOGY DIRECTORATE

Wendel J. Shuely
Robert G. Nickol

SCIENCE APPLICATIONS
INTERNATIONAL CORPORATION
Gunpowder, MD 21010-0068

September 2008

ABERDEEN PROVING GROUND, MD 21010-5424

Disclaimer

The findings in this report are not to be construed as an official Department of the Army position unless so designated by other authorizing documents.

REPORT DOCUMENTATION PAGE

Form Approved
OMB No. 0704-0188

1. REPORT DATE *(DD-MM-YYYY)*	2. REPORT TYPE	3. DATES COVERED *(From - To)*
XX-09-2008	Final	Oct 2001 - Dec 2007

4. TITLE AND SUBTITLE
Evaporation of HD Droplets from Nonporous, Inert Surfaces in TGA Microbalance Wind Tunnels

5a. CONTRACT NUMBER
DAAD13-03-D-0017

5b. GRANT NUMBER

5c. PROGRAM ELEMENT NUMBER

6. AUTHOR(S)
Hong, Seok H.; Sumpter, Kenneth B. (ECBC); Shuely, Wendel J.; and Nickol, Robert G. (SAIC)

5d. PROJECT NUMBER

5e. TASK NUMBER

5f. WORK UNIT NUMBER

7. PERFORMING ORGANIZATION NAME(S) AND ADDRESS(ES)
DIR, ECBC, ATTN: AMSRD-ECB-RT-CM, APG, MD 21010-5424
SAIC, P.O. Box 0068, Gunpowder, MD 21010-0068

8. PERFORMING ORGANIZATION REPORT NUMBER
ECBC-TR-596

9. SPONSORING / MONITORING AGENCY NAME(S) AND ADDRESS(ES)

10. SPONSOR/MONITOR'S ACRONYM(S)

11. SPONSOR/MONITOR'S REPORT NUMBER(S)

12. DISTRIBUTION / AVAILABILITY STATEMENT
Approved for public release; distribution is unlimited.

13. SUPPLEMENTARY NOTES

14. ABSTRACT-LIMIT 200 WORDS
The environmental fate of chemical warfare agents (CWAs) is important because the contact or vapor hazard is critical input for models used to support decisions on the level of individual protection at fixed sites. Two different microbalances, configured in a wind-tunnel geometry, were used to measure the evaporation and desorption rates from surfaces. The overall experimental design covers several neat and thickened agents and several material surfaces. The initial elements of the experimental design reported here include chemical warfare agent HD on inert, nonporous surfaces, [i.e., glass and aluminum, and on an inert, porous surface (i.e., standardized aggregate from concrete and asphalt pavements)]. Two or three environmental temperatures, wind speeds, and relative humidity values were studied.

15. SUBJECT TERMS

CWA	Agent Fate	Environmental Fate	Chemical Warfare Agents	Glass
HD	Mustard	Sessile Droplets	Secondary Evaporation	Surface
Modeling	Desorption	Volatilization	Contact Angle	HPAC
Nonporous	Nonreactive	Evaporation	Bis(2-chloroethyl)sulfide	
VLSTRACK				

16. SECURITY CLASSIFICATION OF:			17. LIMITATION OF ABSTRACT	18. NUMBER OF PAGES	19a. NAME OF RESPONSIBLE PERSON
a. REPORT	b. ABSTRACT	c. THIS PAGE			Sandra J. Johnson
U	U	U	UL	45	19b. TELEPHONE NUMBER *(include area code)* (410) 436-2914

Blank

PREFACE

The work described in this report was authorized under Contract No. DAAD13-03-D-0017. The work was started in October 2001 and completed in December 2007.

The use of either trade or manufacturers' names in this report does not constitute an official endorsement of any commercial products. This report may not be cited for purposes of advertisement.

This report has been approved for public release. Registered users should request additional copies from the Defense Technical Information Center; unregistered users should direct such requests to the National Technical Information Service.

Acknowledgments

The authors thank Daniel Weber and John Molnar, U.S. Army Edgewood Chemical Biological Center (ECBC) for glass disc preparation and Dr. David Tevault, ECBC, for many helpful discussions. They also acknowledge the managerial support provided by Drs. Terrence G. D'Onofrio, H. Dupont Durst, James Savage; and Lawrence Bickford, ECBC, and Drs. David Stockwell, S. Bosco; and Fred Crowson (Defense Threat Reduction Agency, Fort Belvoir, VA). The authors are also grateful to Christine Franklin (SAIC, Abingdon, MD), and Kristina Dressler (Booz Allen Hamilton, Belcamp, MD) for administrative assistance.

Blank

CONTENTS

FIGURES

TABLES

EVAPORATION OF HD DROPLETS FROM NONPOROUS, INERT SURFACES IN TGA MICROBALANCE WIND TUNNELS

1. INTRODUCTION

The environmental fate of chemical warfare agents (CWAs) on targeted surfaces is important in modeling vapor and contact hazard for decisions influencing safety of personnel in contaminated areas. The goal is to provide data sets to allow development of improved models for hazard predictions, supporting decisions on personnel safety. The main objective of this study is to provide fundamental understanding of agent evaporation/desorption as a function of material variables as well as environmental variables. Chemical warfare agent droplets on a surface either evaporate or sorb into the surface material, then desorb at slower, diffusion controlled rates.[1] The rates of these processes determine the environmental fate of CWAs, and these rates are important because the contact and vapor hazard are critical input for models used to support decisions on the level of individual protection at fixed sites.[2] Table 1 shows possible agents and surfaces.

Table 1. Possible CW Agents and Surfaces

CW Agent	Surface	
	Control (Laboratory)	Real World
HD	Glass	Concrete
GD	Aluminum	Asphalt
VX	Teflon	Sand/Soil
Thickened	Aggregate	Vegetation
	Mortar	

A drop of agent on a surface will evaporate. There are two possible mechanisms: (1) the drop maintains constant contact angle, and (2) the drop maintains constant contact area. If a drop maintains constant contact angle, the rate of evaporation changes throughout the process because the surface area changes as the evaporation proceeds as shown in Figure 1. On the other hand, if the drop maintains constant contact area, the surface area should not change much throughout the process; therefore, the rate of evaporation remains constant (also shown in Figure 1). Chemical warfare agent can also diffuse through the pores of the surface and slowly diffuse back out to evaporate, providing the surface is porous and chemically inert. These rates are a function of material variables (e.g., chemical vapor pressure, the drop size, the pore size, and the surface substrate). They are also a function of environmental variables such as temperature, relative humidity (RH), and wind speed.

Two different microbalances, TA Instrument TGA 2950 and SDT Q600 configured in a wind tunnel geometry, were used to measure the evaporation and desorption rates from surfaces. The TA Model SDT Q600 is a dual beam, horizontal microbalance with

Text continues on page 16.

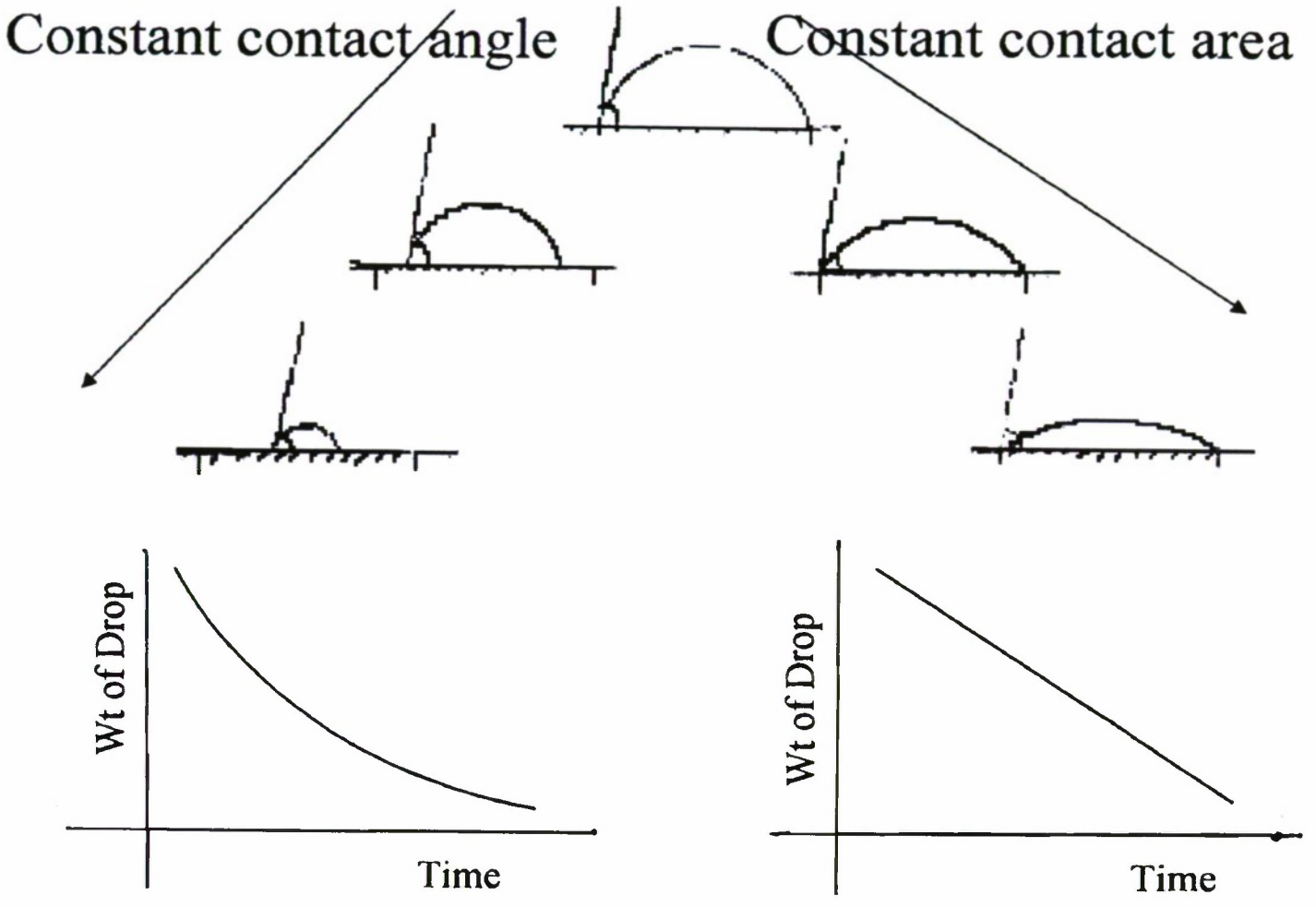

Figure 1. Schematic Representation of HD Evaporation Process from Inert, Nonporous Surface.

Figure 2. TA Model Q600 Simultaneous DSC-TGA Used in Microbalance Wind Tunnel Studies.

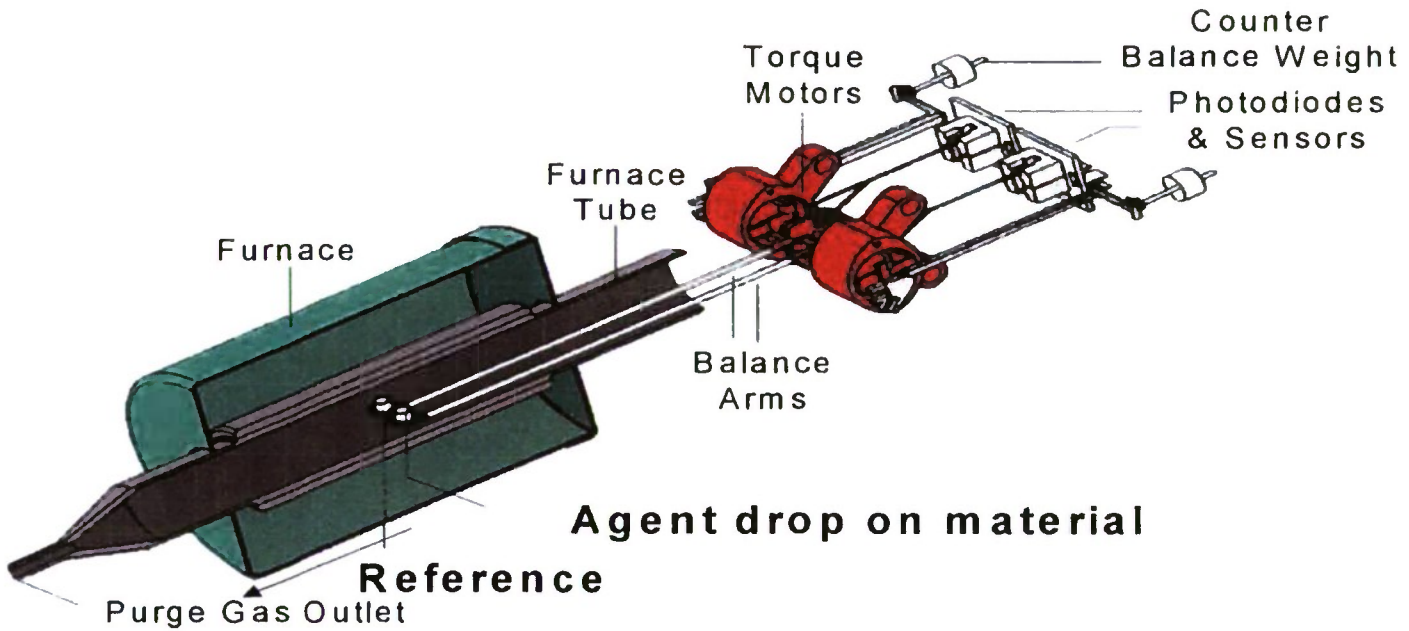

Figure 3. Microbalance Wind Tunnel Based on Horizontal Dual Beam Geometry (TA Model Q600).

Figure 4. Vertical Microbalance with Evolved Gas Analysis Option for the TA Model 2950 Allowing its Use as a Horizontal Wind Tunnel

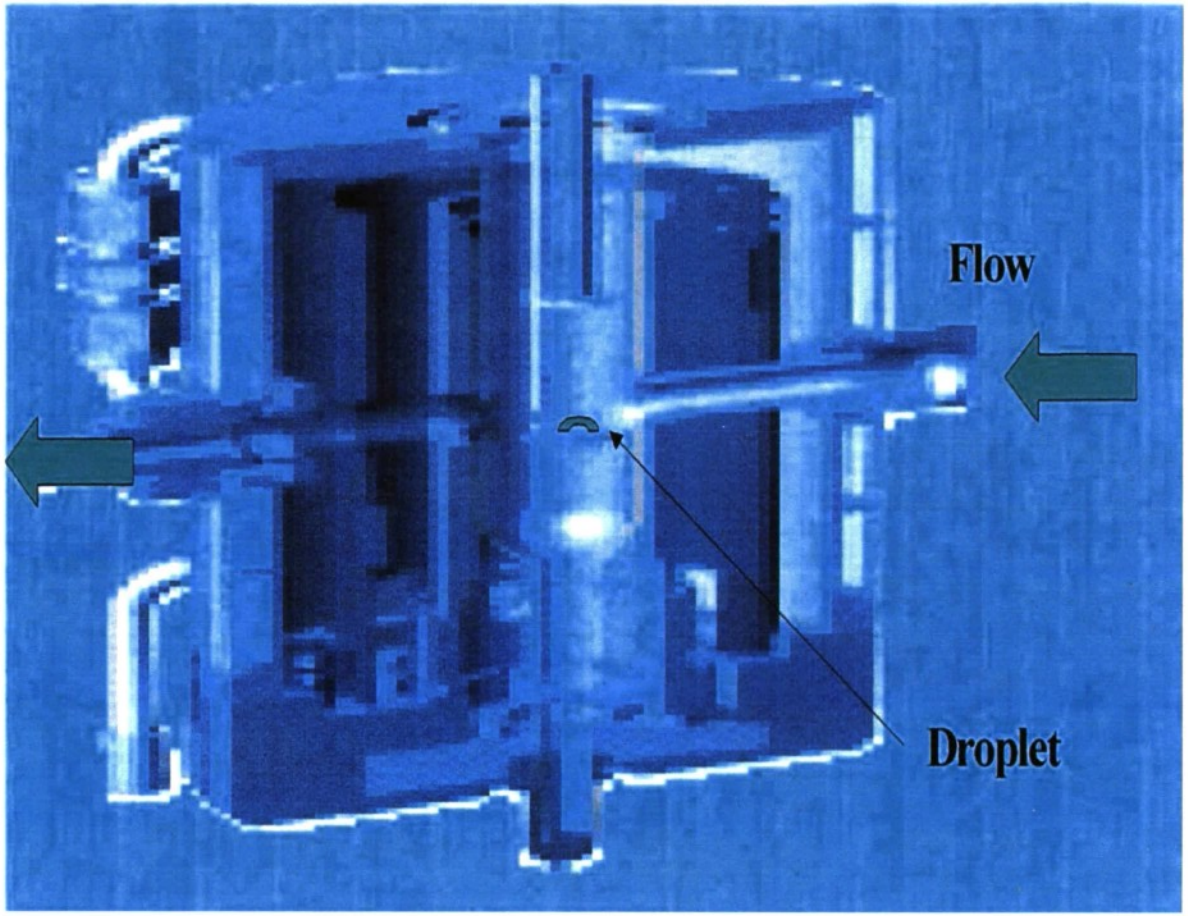

Figure 5. Horizontal Wind Tunnel Mode of TA Model 2950 Microbalance Based on Evolved Gas Analysis Geometry.

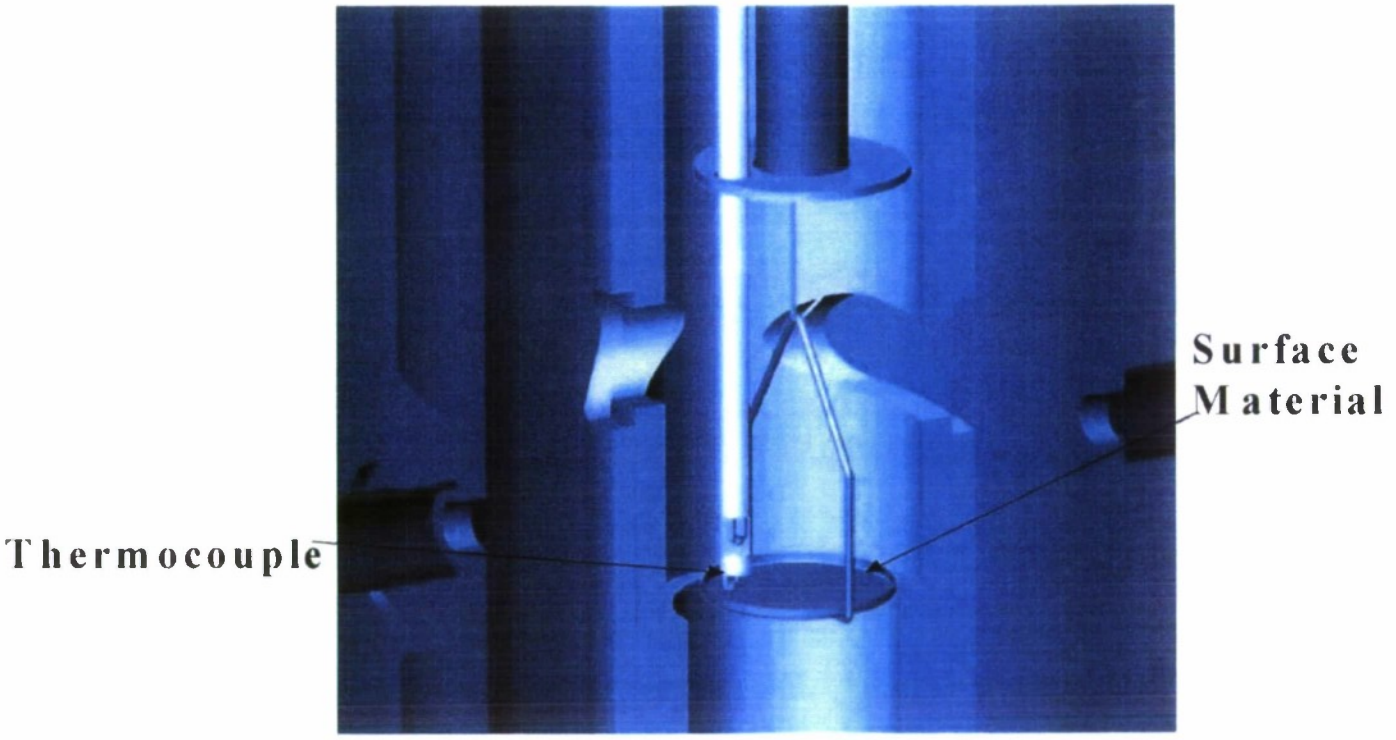

Figure 6. Material Surface on Microbalance Wind Tunnel Sample Holder and Sample/Control Thermocouple: TA Model 2950.

simultaneous differential thermal analysis system, and TA Model TGA-2950 is a vertical microbalance with evolved gas geometry (Figures 2-6). The chemical agent, HD, was placed on several different surface materials, which are not chemically reactive with HD and also not porous. They are Aluminum 2024, Glass, and Teflon. The weight loss (evaporation) rates were measured under different conditions. One of the surface materials, Aluminum 2024, is from the unpainted floor of a C17 Cargo Aircraft.* After each measurement, residual CWA was analyzed using GC/MSD.

The methods used here are also applicable to agent fate within building interiors. The rates were also measured as a function of environmental variables, such as temperature, RH, and wind speed. The weight-loss *versus* time plots were overlaid to allow comparison of the rates under various conditions.

2. EXPERIMENTATION

2.1 Materials

The purity of HD used was 90+% by GC/TCD. The reference nonporous materials used were 2024 Aluminum, Teflon, and glass. The concrete was standardized for the program, and the composition of the concrete and its components has been documented.[3]

2.2 Instrumentation

Microbalance wind tunnels were adapted from thermogravimetric analyzers (TGA). The TA Instrument Model TGA-2950 vertical microbalance was used in evolved gas analysis (EGA) mode to produce a horizontal wind tunnel geometry. The dual beam, horizontal microbalance with simultaneous differential thermal (SDT) analysis (TA Model SDT-Q600) was used as the microbalance wind tunnel. The residual CWA was analyzed using GC/MSD.

A photo of the horizontal microbalance is shown in Figure 2. The motorized temperature control chamber is shown in the Open position, and the two balance beams are exposed for loading the chemical agent drop onto a material surface on the sample holder.

A diagram of the dual beam balance is shown in Figure 3. The flow is from right to left. The sample and reference holder are shown at the end of the two beams. The furnace tube provides a cylindrical ceramic wind tunnel around the contaminant droplet on the material surface.

The vertical microbalance TA Instruments Model TGA-2950 is shown in the Open position in Figure 4. The EGA fixture is shown installed in Figure 5.

* Private communication with Tim Provens, Wright-Patterson AFB, Wright-Patterson, OH.

The flow direction from right to left is indicated along with a superimposed diagram of a contaminant droplet on a material surface (not to scale). A close-up diagram provided in Figure 6 shows the holder for the surface material and the measurement and control thermocouple close to the material surface.

Temperature and RH are controlled by a humidity generator (Thunder Scientific Corporation Model 2500, Albuquerque, NM).

2.3 Surface Preparation

Glass and Teflon discs were cleaned by the following procedure: the disc was submerged in concentrated HNO_3 (65%) for 24 hr (lightly swirled on a rotating plateau). Then, the glass was rinsed with dematerialized water and dried (using appropriate fat-free non-felting paper towels). Subsequently, the disk was rinsed shortly with 99% PA hexane and wiped dry (using appropriate fat-free non-felting paper towels).

2.4 Conditions

The influential factors that can affect evaporation/desorption rates, other than the intrinsic properties of droplets and surfaces, are temperature, humidity, and wind speed. The temperatures of interest are the droplet temperature, the substrate temperature, and the air temperature.[4] According to a statistical consideration using meteorological data, the temperature set to be studied was 15 °C, 40 °C, and 55 °C. The initial study used the flow rate of 100 mL/min, and later 500, and 1000 mL/min.[5]

3. RESULTS AND DISCUSSION

Examples of evaporation and/or desorption measurements results are provided in Figures 7 through 16. All plots have droplet weight on the y-axis and time on the x-axis. All of these interim plots have been neither normalized nor filtered into their final format. In all cases, individual experiments have been combined and overlaid onto a single plot to allow comparisons. The preliminary wind speeds noted were mean values based on flow rate and cross-sectional area; the wind speed at the drop surface interface is being determined and reported separately.[4,6,7]

3.1 HD on Aluminum Surface

The evaporation rates of HD from aluminum are shown in Figure 7; two repetitions each are shown for target drop sizes of 0.5, 1, and 2 mg. The time to complete evaporation increases systematically from about 210 to about 650 min (factor of 3.1x) as the drop size increases from 0.5 to 2 mg (factor of 4x). There is a slight decrease in rate (from 4.4 µg/min to 3.0 µg/min) with decreasing drop size, perhaps due to a smaller surface area for smaller HD drops on aluminum. The results are summarized in Table 2.

Text continues on page 28.

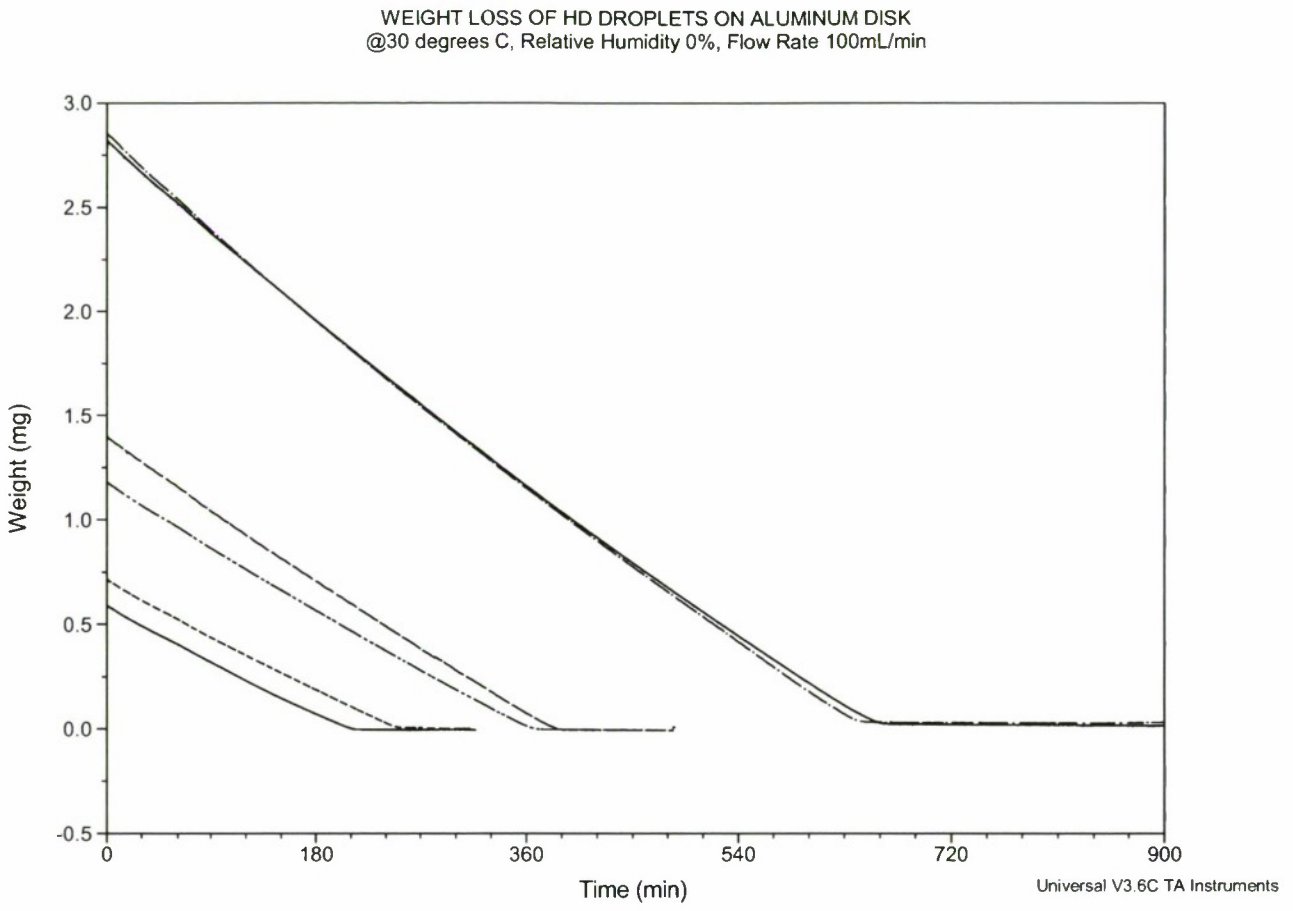

Figure 7. Comparison of HD Evaporation Rate from Aluminum: @ 30 °C, 0% RH, and 100 mL/min Flow Rate.

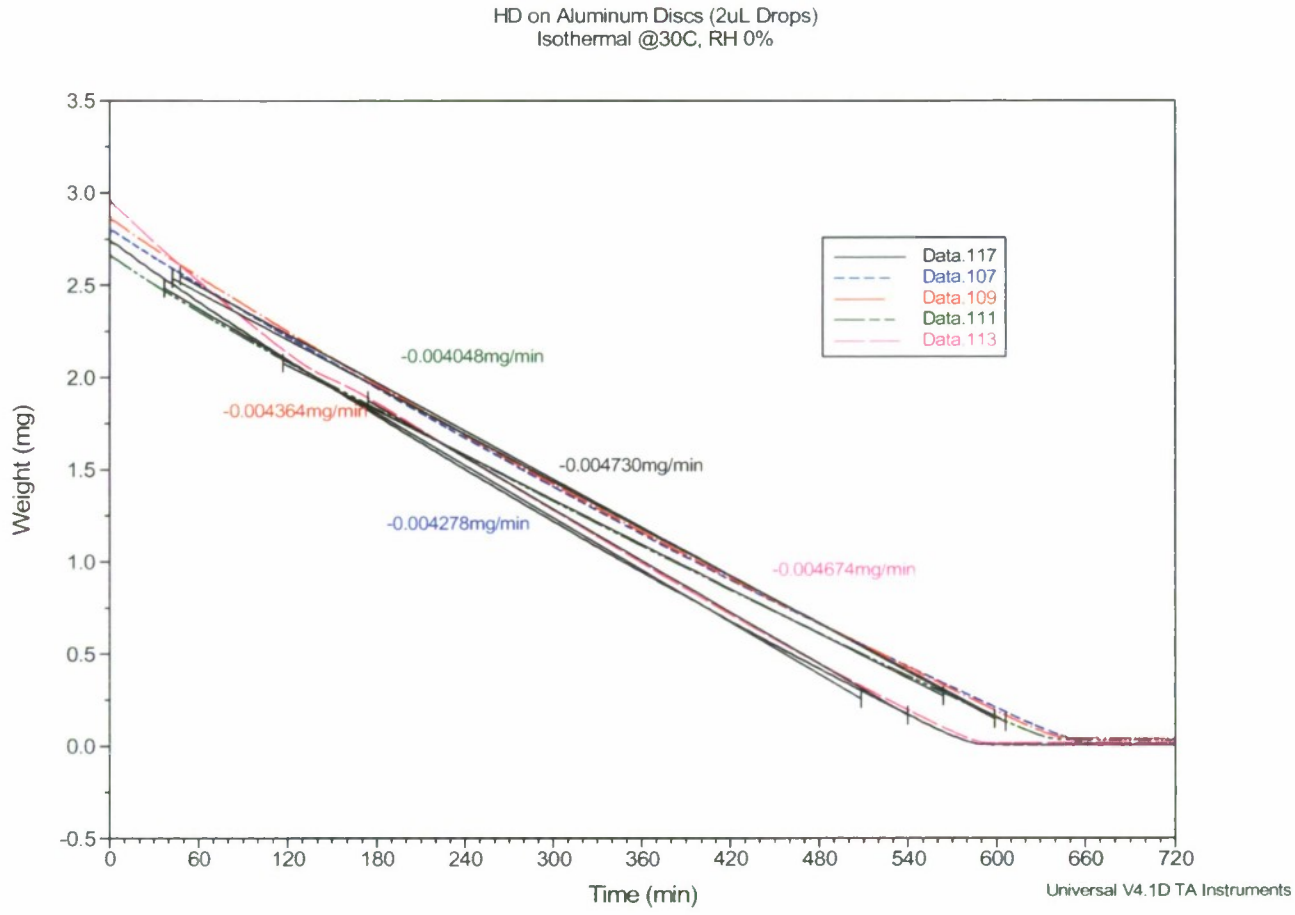

Figure 8. Comparison of HD Evaporation Rate from Aluminum: @ 30 °C, 0% RH, and 100 mL/min Flow Rate.

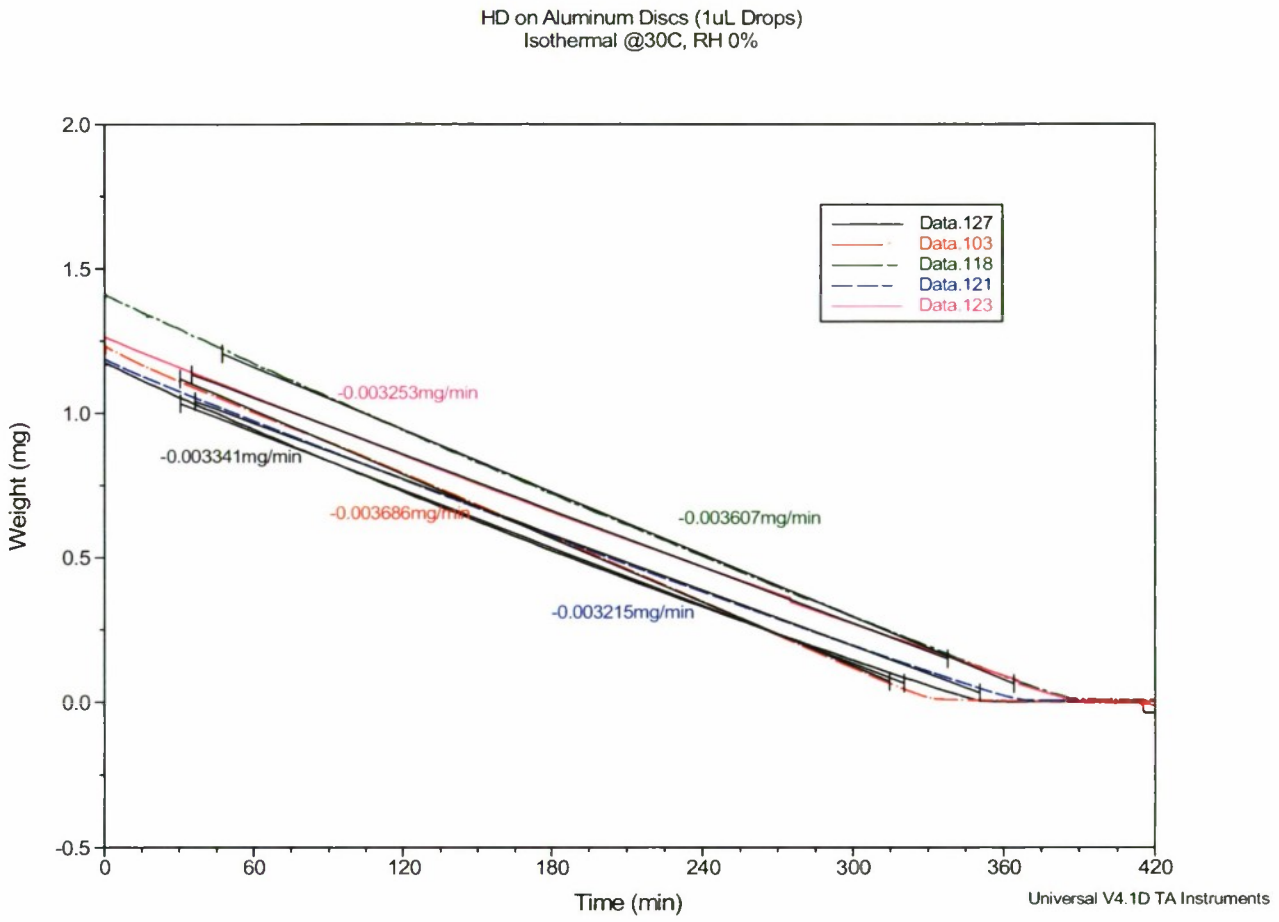

Figure 9. Comparison of HD Evaporation Rate from Aluminum: @ 30 °C, 0% RH, and 100 mL/min Flow Rate.

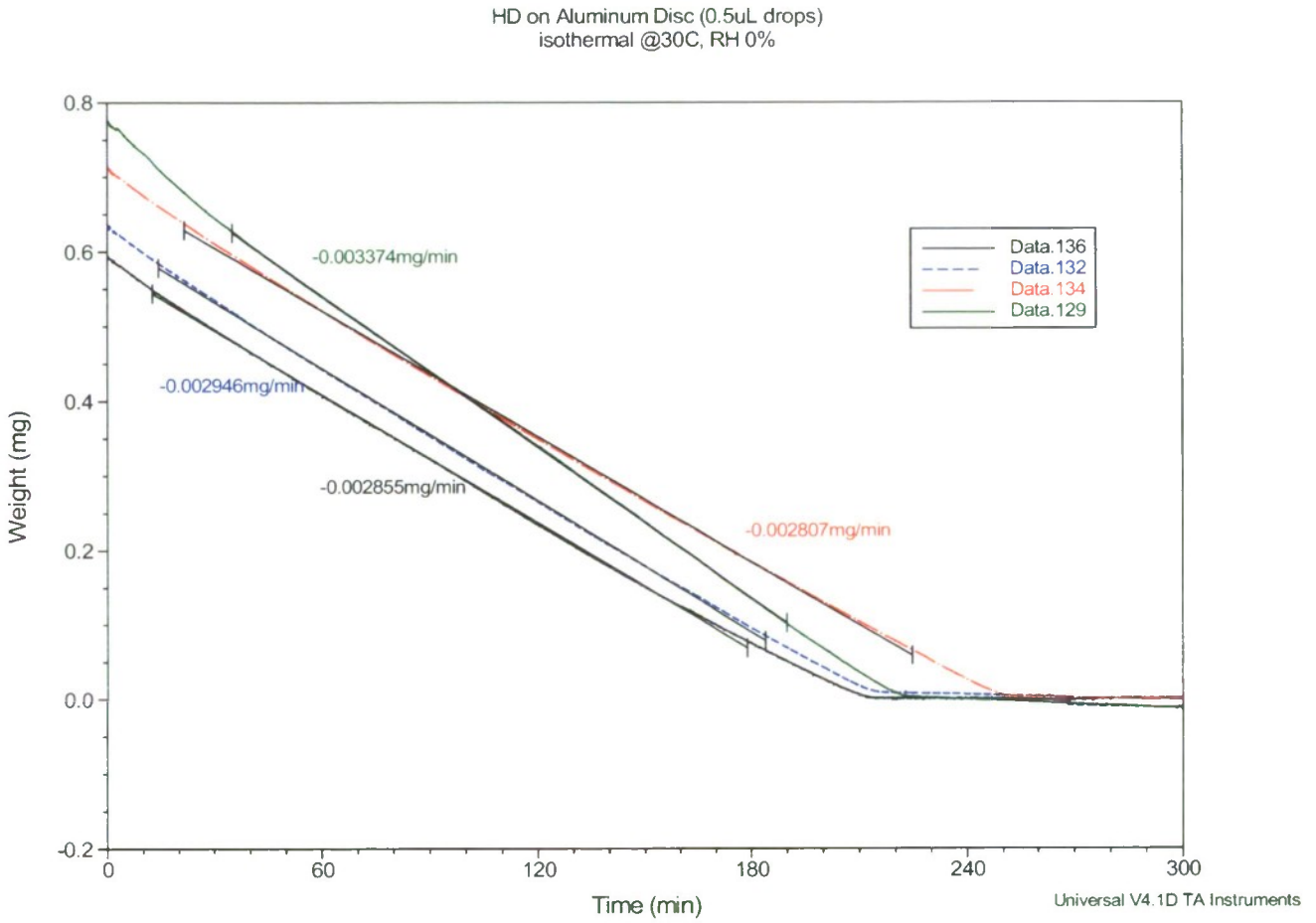

Figure 10. Comparison of HD Evaporation Rate from Aluminum: @ 30 °C, 0% RH, and 100 mL/min Flow Rate.

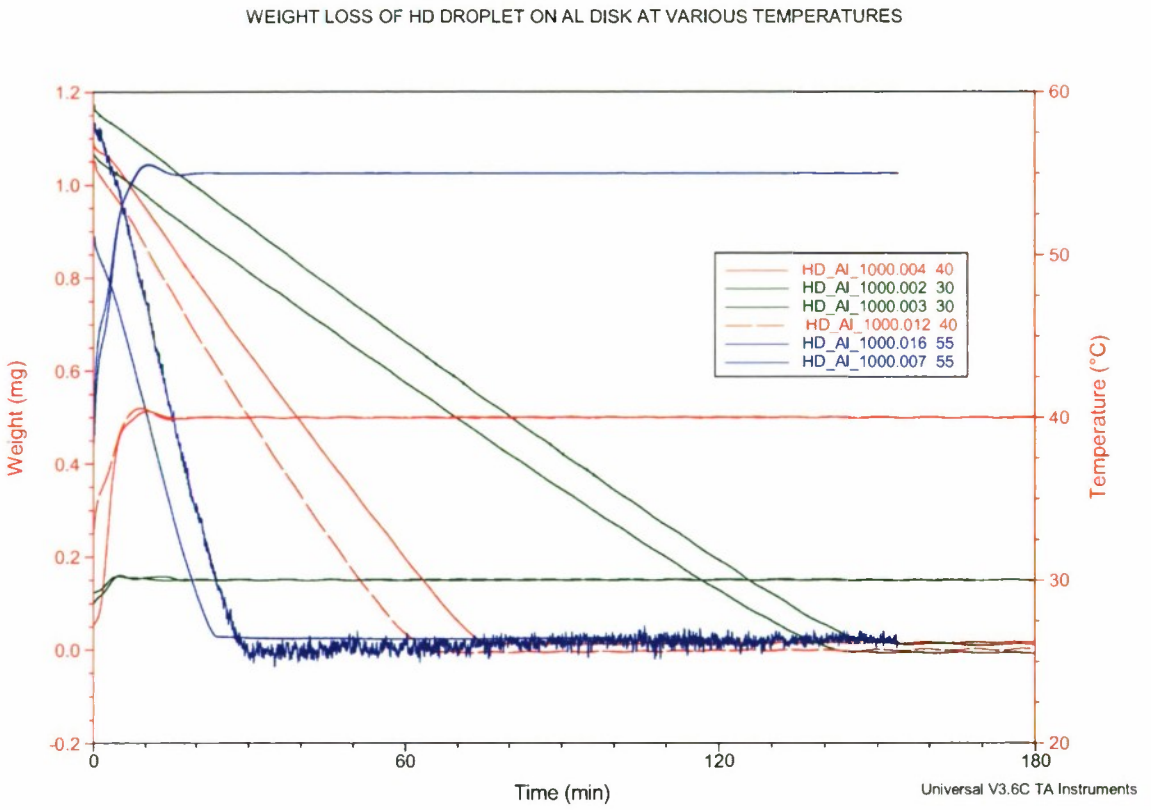

Figure 11. Comparison of HD Evaporation Rate from Aluminum at Various Temperatures: 0% RH and 1000 mL/min Flow Rate.

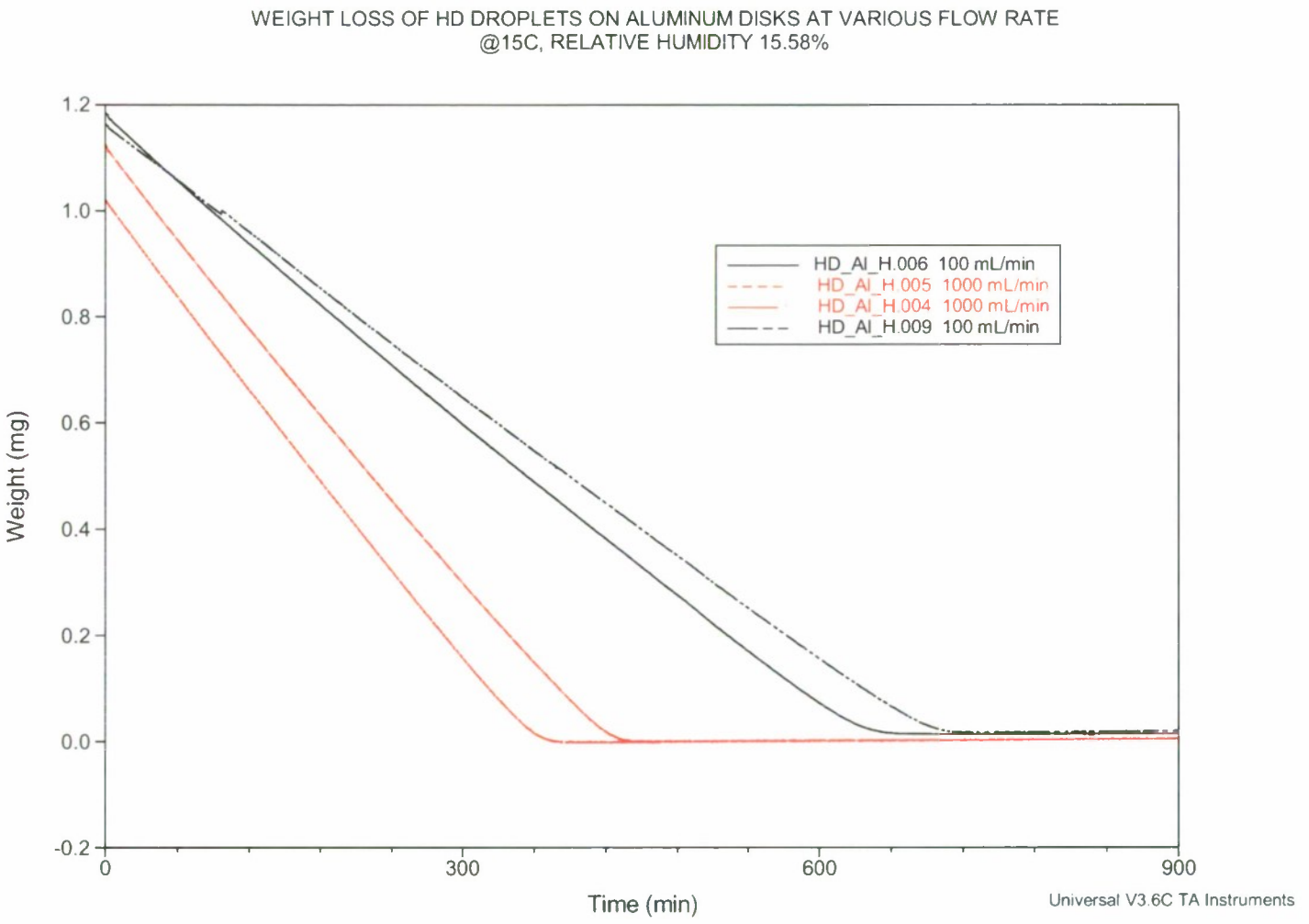

Figure 12. Comparison of HD Evaporation Rate from Aluminum at Various Flow Rates: @ Ambient Temperature and 15.58% RH.

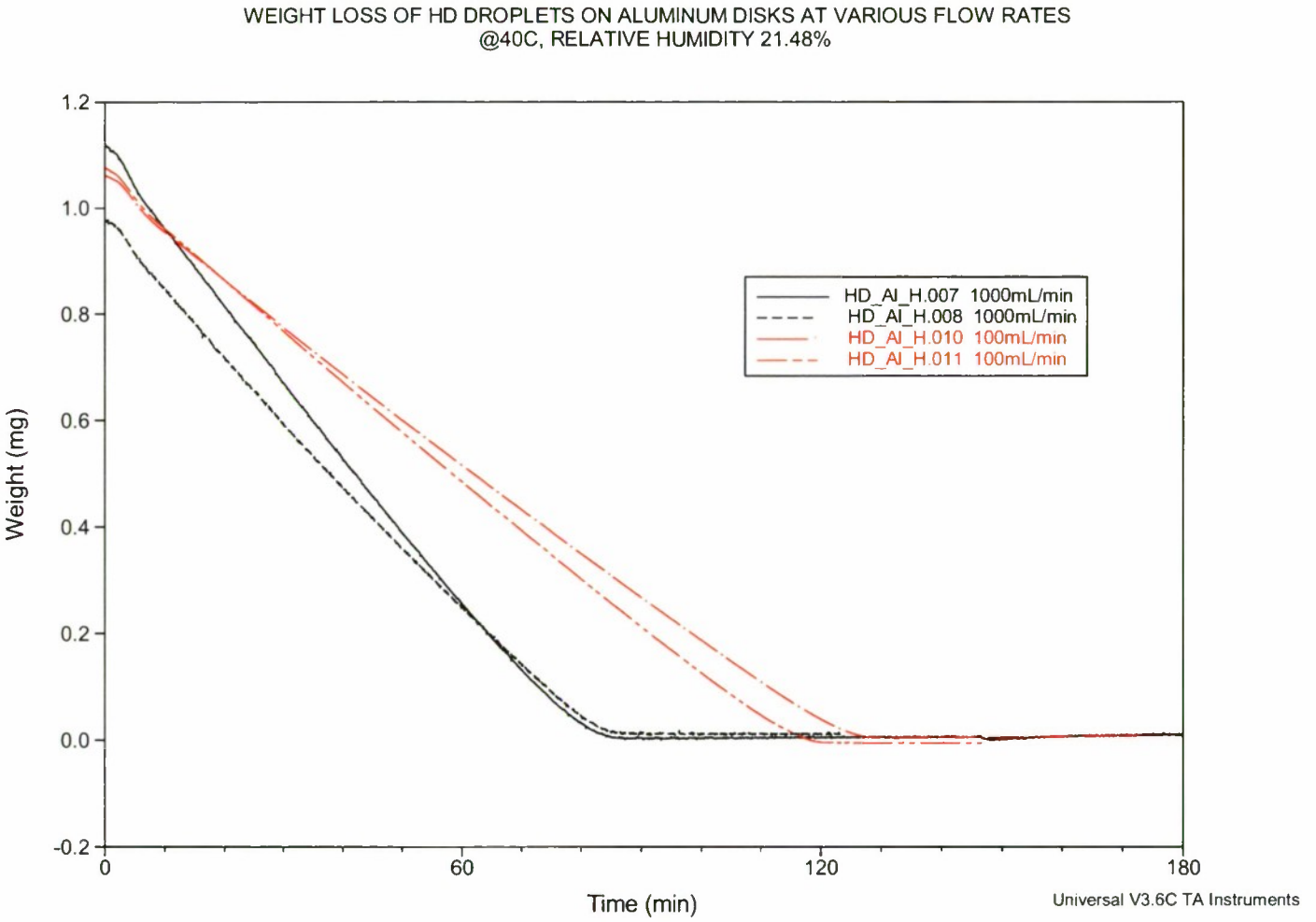

Figure 13. Comparison of HD Evaporation Rate from Aluminum at Various Flow Rates: @ 40 °C and 21.48% RH.

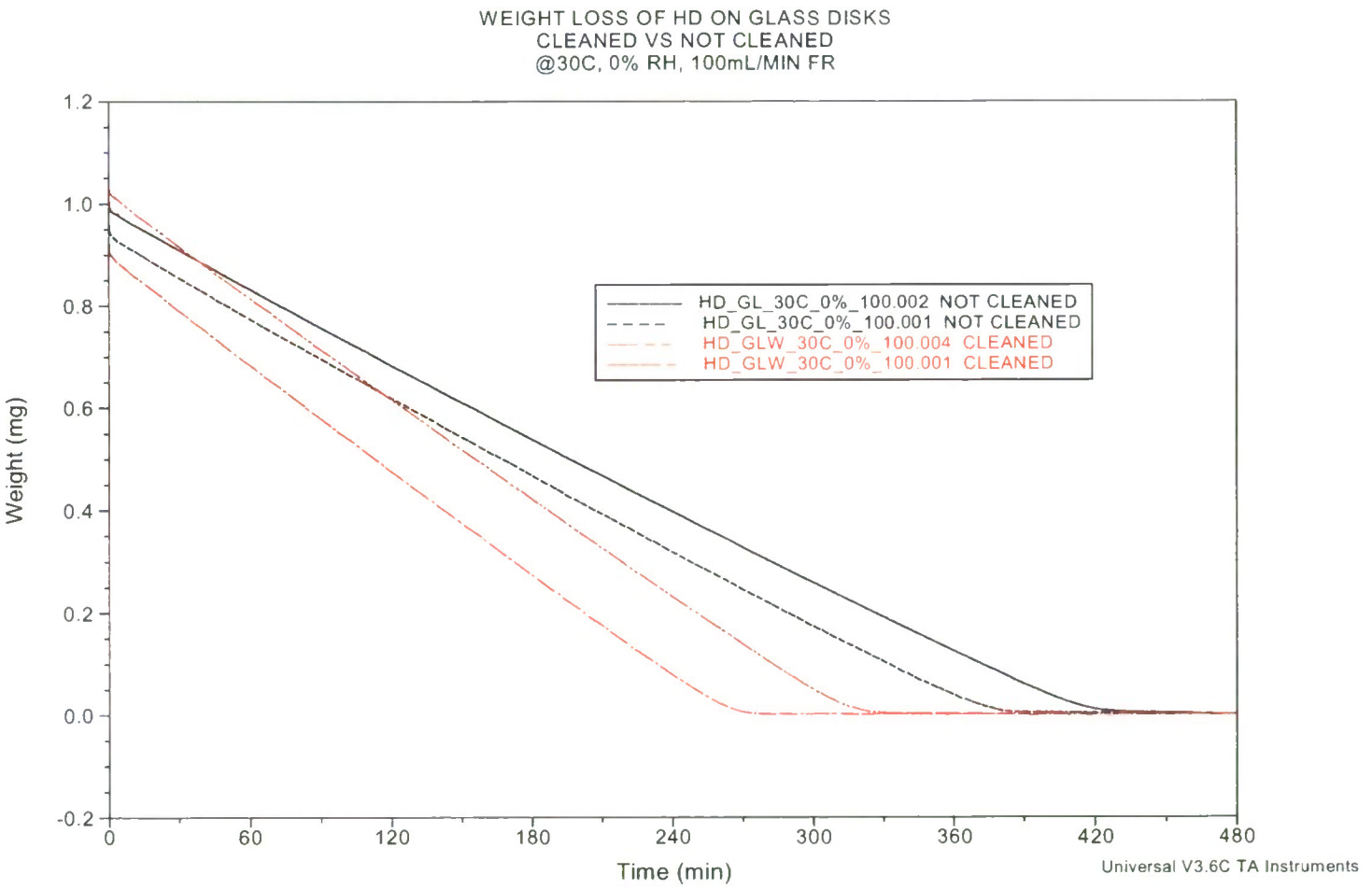

Figure 14. Comparison of HD Evaporation Rate from Glass (Cover): Cleaned vs. Uncleaned @ 30 °C, 0% RH, and 100 mL/min Flow Rate.

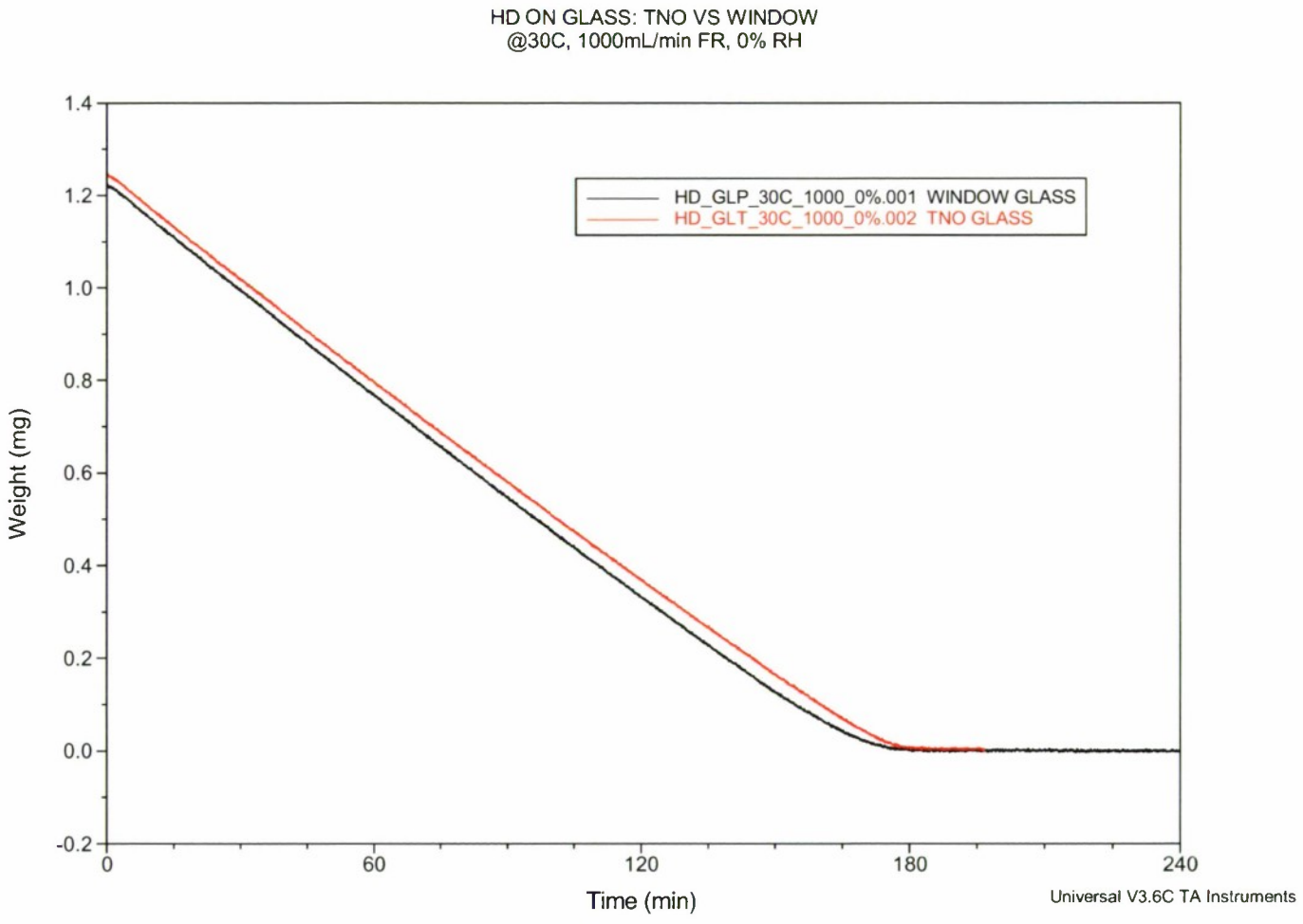

Figure 15. Comparison of HD Evaporation Rate from Glass TNO Glass vs. Window Glass (both cleaned) @ 30 °C, 0% RH, and 100 mL/min Flow Rate.

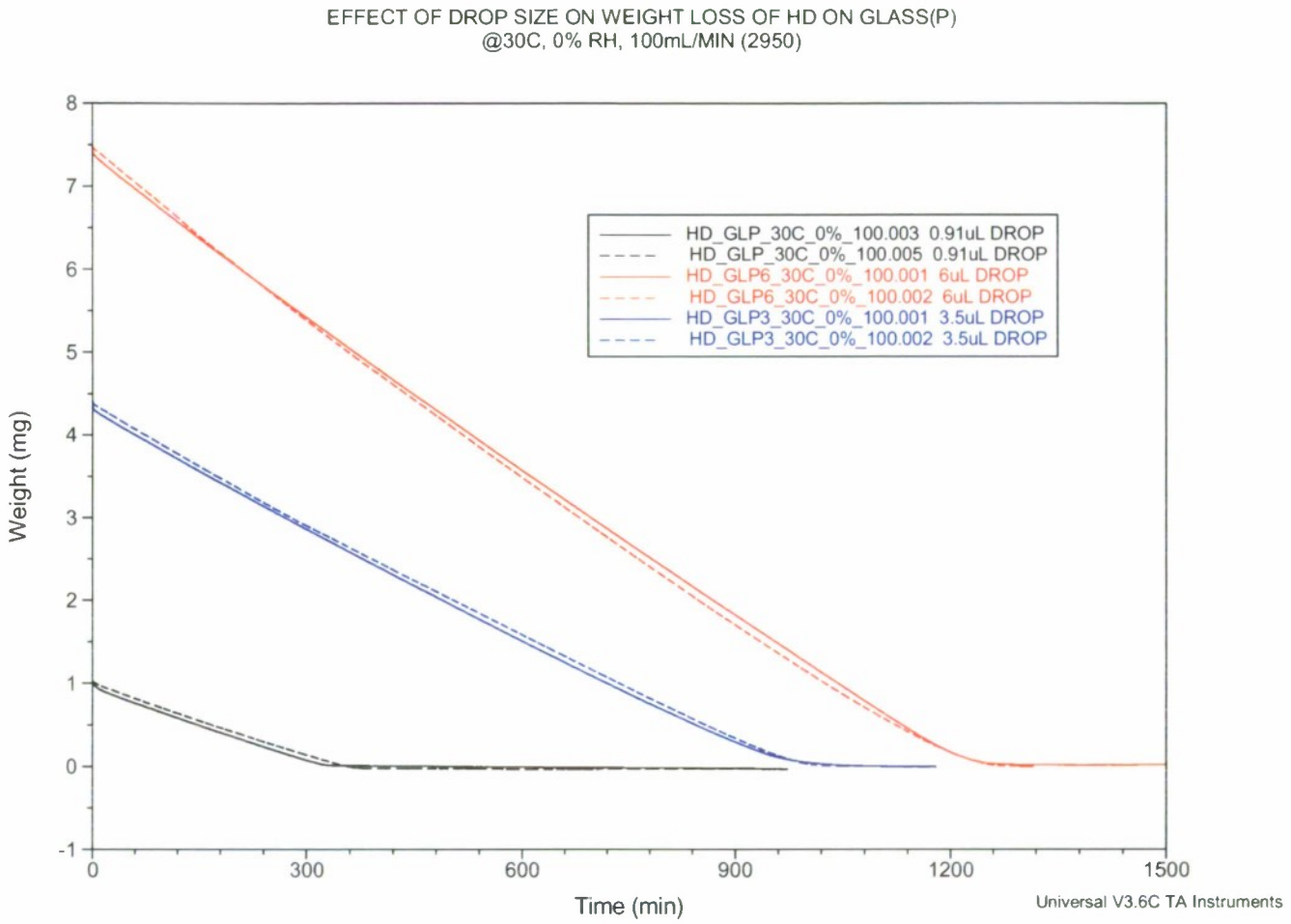

Figure 16. Comparison of HD Evaporation Rate from Glass (Window) from Various Drop Sizes: @ 30 °C, 0% RH, and 100 mL/min Flow Rate.

Table 2. Evaporation Rates of HD Droplets from Aluminum Surface Measured by Microbalance Wind Tunnel (TGA) at 30 °C and 0% RH.

Run No.	Evaporation Rate by TGA (µg/min)	Dropsize (µL)	Ave. Rate (µg/min)	Figure
129	3.374	0.5	2.996 ± 0.259	8
132	2.946			
134	2.807			
136	2.855			
103	3.686	1.0	3.420 ± 0.213	9
118	3.607			
121	3.215			
123	3.253			
127	3.341			
107	4.278	2.0	4.419 ± 0.284	0
109	4.364			
111	4.048			
113	4.674			
117	4.730			

Five repetitions for HD evaporation from aluminum are plotted for droplets of approximately 1.6 mm spherical diameter or 2.0 µL in volume (Figure 8). The measurements show good reproducibility and time to completc evaporation at about 10 to 11 hr. The ability of the operator to reproduce the targeted drop size at the 2-3 mg level was quite good, ranging about 0.15 mg or a 5% range. Figure 9 shows evaporation rate of 1 µL drops of HD (approximately 1.2 - 1.45 mg) from aluminum. At the targeted drop size of 0.5 µL or 0.62 mg (Figure 10), a range of drop masses from 0.57 to 0.75 mg (about 0.47 - 0.6 µL) were deposited on glass discs. These three figures show the difficulty in deposition of targeted drop sizes as the drops become smaller. However, the microbalance wind tunnels have the advantage that the actual drop size deposited is measured, regardless of the target drop size. Our other methods for other environmental fate experiments still need to overcome this procedural difficulty. The drop masses varied by a factor of about 1.3x, and the time to complete evaporation varied by about 1.16x (250/215 min).

Figure 11 shows the weight loss of HD droplets on aluminum disks at various temperatures (i.e., 30, 40, and 55 °C). As expected, at higher temperature, the rate of weight loss was greater. Figures 12 and 13 show the weight loss of HD droplets at two different flow rates. Again, as expected, at higher flow rates, the rate of weight loss was greater. These results are summarized in Table 3.

Table 3. Evaporation Rates of HD Droplets from Aluminum Surface under Various Conditions Measured by Microbalance Wind Tunnel (TGA).

Run No.	Evaporation Rate by TGA (μg/min)	Temp. (°C)	Ave. Rate (μg/min)	Flow Rate (mL/min)	RH (%)	Instrument
1	7.441	30	7.709 ± 0.379	1000	0	TGA2950
2	7.977					
3	7.691					
10	17.29	40	17.42 ± 0.905			
11	16.61					
12	17.07					
13	18.71					
14	18.19					
7	22.13	55	34.60 ± 10.94			
8	39.10					
16	42.57					
H4	2.629	Amb. (~20)	2.734 ± 0.148	1000	15.6	SDT Q600
H5	2.839					
H6	1.830		1.755 ± 0.107	100		
H9	1.679					
H7	13.86	40	12.74 ± 1.584	1000	21.5	
H8	11.62					
H10	8.418		8.826 ± 0.577	100		
H11	9.234					
H12	26.47	55	27.22 ± 1.061	100	10.5	
H13	27.97					
H14	49.34		49.34	1000		

3.2 HD on Glass

The evaporation rates of HD from a glass surface are shown in Figure 14. Two repetitions each are shown for the cover glass with and without cleaning. There is a slight change in rate with cleaning, perhaps due to removal of any existing dirt or grease spots from the glass surface, which could cause either a different contact angle or a different drop shape. However, when two different types of glass discs were used (both cleaned with the same procedure), the evaporation rates were almost identical to those shown in Figure 15.

Figure 16 shows the evaporation rates of HD from glass (window). Two repetitions each are shown for target drop sizes of 1, 3.5, and 6 μL. The time to complete evaporation increases systematically from about 360 to about 1300 min (factor of 3.6x) as the drop size increases from 1 to 6 μL (factor of 6x). Figure 17 also shows the evaporation rates of HD from glass (TNO). The results were similar to those obtained with window glass. In both cases, there is an increase in rate with increasing drop size, perhaps due to a larger surface area for larger HD drops on glass. The results are summarized in Table 4.

Table 4. Evaporation Rates of HD Droplets from Glass Surface Measured by Microbalance Wind Tunnel (TGA) at 30 °C and 0% RH.

Run No.	Evaporation Rate by TGA (μg/min)	Dropsize (μL)	Ave. Rate (μg/min)	Flow Rate (mL/min)
GLP1001	2.527	1.0	2.746 ± 0.192	100
GLP1003	2.887			
GLP1005	2.824			
GLP3001	4.446	3.5	4.403 ± 0.061	
GLP3002	4.360			
GLP6001	5.968	6.0	6.089 ± 0.171	
GLP6002	6.210			
GLT1001	5.463	1.0	5.028 ± 0.306	1000
GLT1002	4.971			
GLT1003	4.747			
GLT1004	4.930			
GLT3001	8.433	3.5	9.575 ± 1.392	
GLT3002	10.73			
GLT3003	8.309			
GLT3004	10.83			
GLT6001	14.97	6.0	12.58 ± 1.684	
GLT6002	12.76			
GLT6003	11.82			
GLT6004	10.37			
GLT6005	12.96			

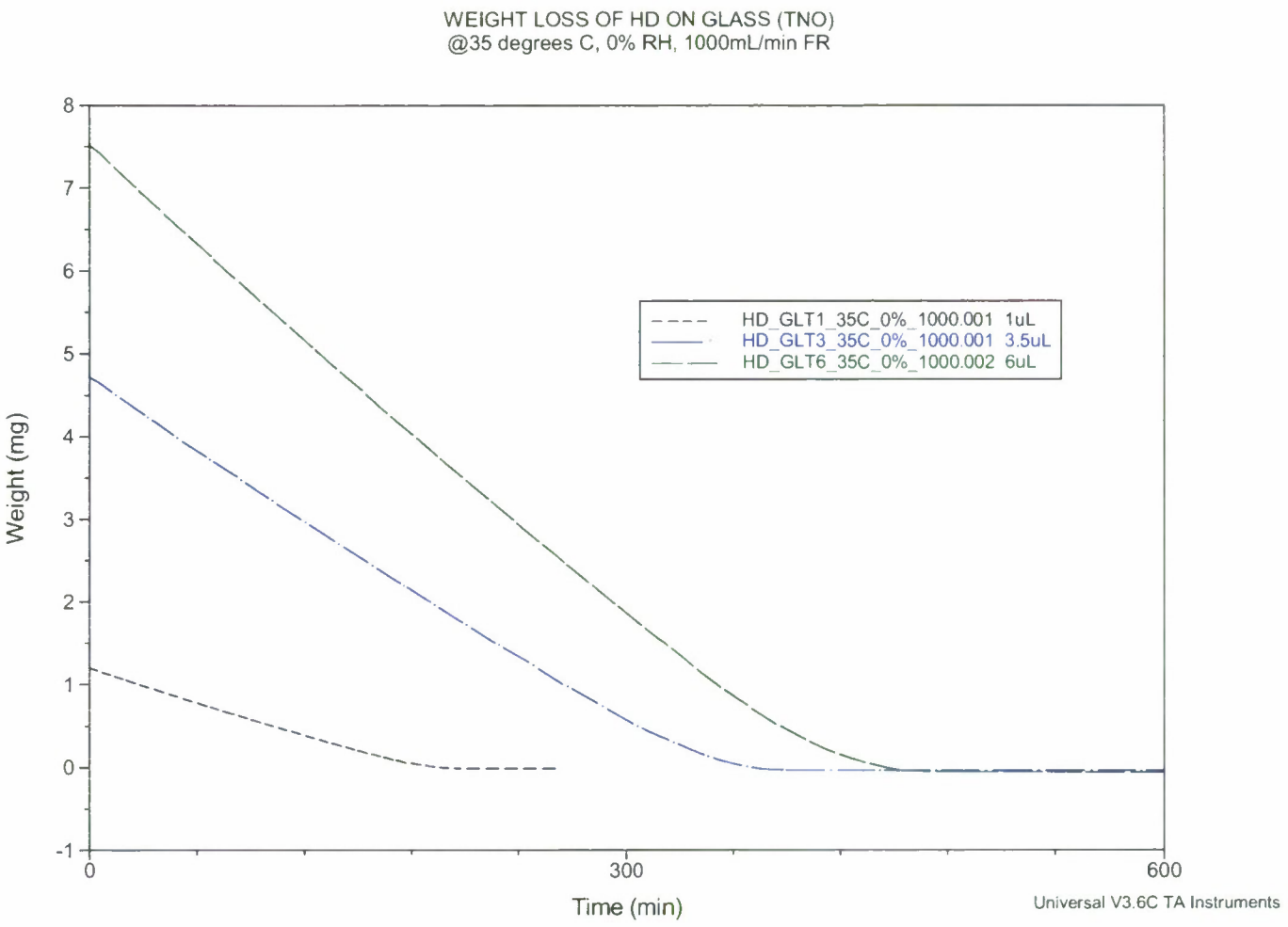

Figure 17. Comparison of HD Evaporation Rate from Glass (TNO): Drop Size Effect @ 35 °C, 0% RH, and 1000 mL/min Flow Rate.

Figures 18 and 19 show the weight loss of HD droplets from glass discs at various temperatures (i.e., 30, 40, and 55 °C). As expected, at higher temperatures, the rate of weight loss was greater. Figures 20 and 21 show the weight loss of HD droplets at different flow rates. Again, as expected, at higher flow rates, the rate of weight loss was greater. Figure 22 shows the weight loss of HD droplets at three different RHs. It is apparent that the humidity has little, if any, influence to the evaporation of HD under these conditions. These results are summarized in Table 5.

Table 5. Evaporation Rates of HD Droplets from Glass Surface under Various Conditions Measured by Microbalance Wind Tunnel (TGA).

Run No.	Evaporation Rate by TGA (μg/min)	Temp. (°C)	Ave. Rate (μg/min)	Flow Rate (mL/m)	RH (%)	Instrument (Figure)
GLP3001	2.524	30	2.568 ± 0.382	100	0	TGA2950 (18)
GLP3002	2.045					
GLP3003	2.879					
GLP3005	2.823					
GLP4001	6.759	40	6.063 ± 0.630			
GLP4002	5.531					
GLP4003	5.899					
GLP5501	17.34	55	18.52 ± 1.836			
GLP5502	19.96					
GLP5503	17.19					
GLP5504	21.01					
GLP5505	17.09					
GLT3001	7.744	30	7.467 ± 0.392	1000	0	SDT Q600 (19)
GLT3002	7.189					
GLT4001	13.92	40	15.83 ± 1.753			
GLT4002	17.96					
GLT4003	15.01					
GLT4004	16.43					
GLT5501	51.63	55	48.70 ± 3.422			
GLT5502	46.28					
GLT5503	45.23					
GLT5504	51.64					
GLP100-1	6.773	40	6.052 ± 0.649	100	0	TGA2950 (20)
GLP100-2	5.515					
GLP100-3	5.869					
GLP1000-1	9.892		10.08 ± 0.260	1000		
GLP1000-2	10.26					

Table 5. Evaporation Rates of HD Droplets from Glass Surface under Various Conditions Measured by Microbalance Wind Tunnel (TGA). (Continued)

Run No.	Evaporation Rate by TGA (µg/min)	Temp. (°C)	Ave. Rate (µg/min)	Flow Rate (mL/m)	RH (%)	Instrument (Figure)
GLT10-1	3.124	30	3.065 ± 0.148	10	0	SDT Q600 (21)
GLT10-2	3.174					
GLT10-3	2.896					
GLT100-1	3.814		3.814	100		
GLT500-1	5.222		5.241 ± 0.026	500		
GLT500-2	5.259					
GLT1000-1	7.744		7.432 ± 0.442	1000		
GLT1000-2	7.119					
GLP00-1	11.64	40	12.51 ± 1.734	500	0	SDT Q600 (22)
GLP00-4	11.57					
GLP00-5	15.57					
GLP00-6	11.54					
GLP00-7	12.22					
GLP21-1	11.86		12.17 ± 0.438		21.5	
GLP21-2	12.48					
GLP45-1	12.95		12.39 ± 0.792		44.9	
GLP45-2	11.83					

Text continues on page 39.

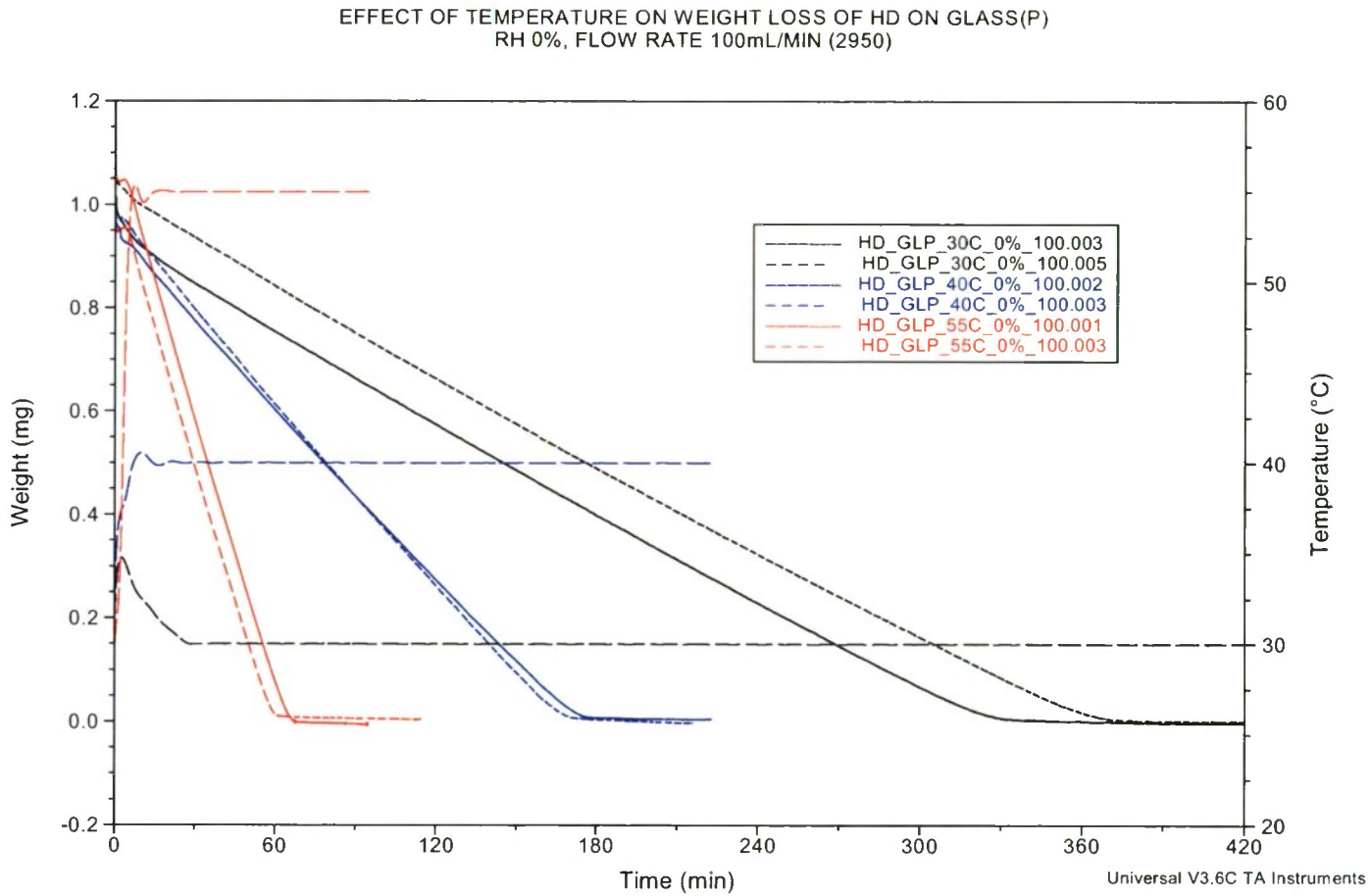

Figure 18. Comparison of HD Evaporation Rate from Glass (Window) at Various Temperatures: 0% RH and 100 mL/min Flow Rate.

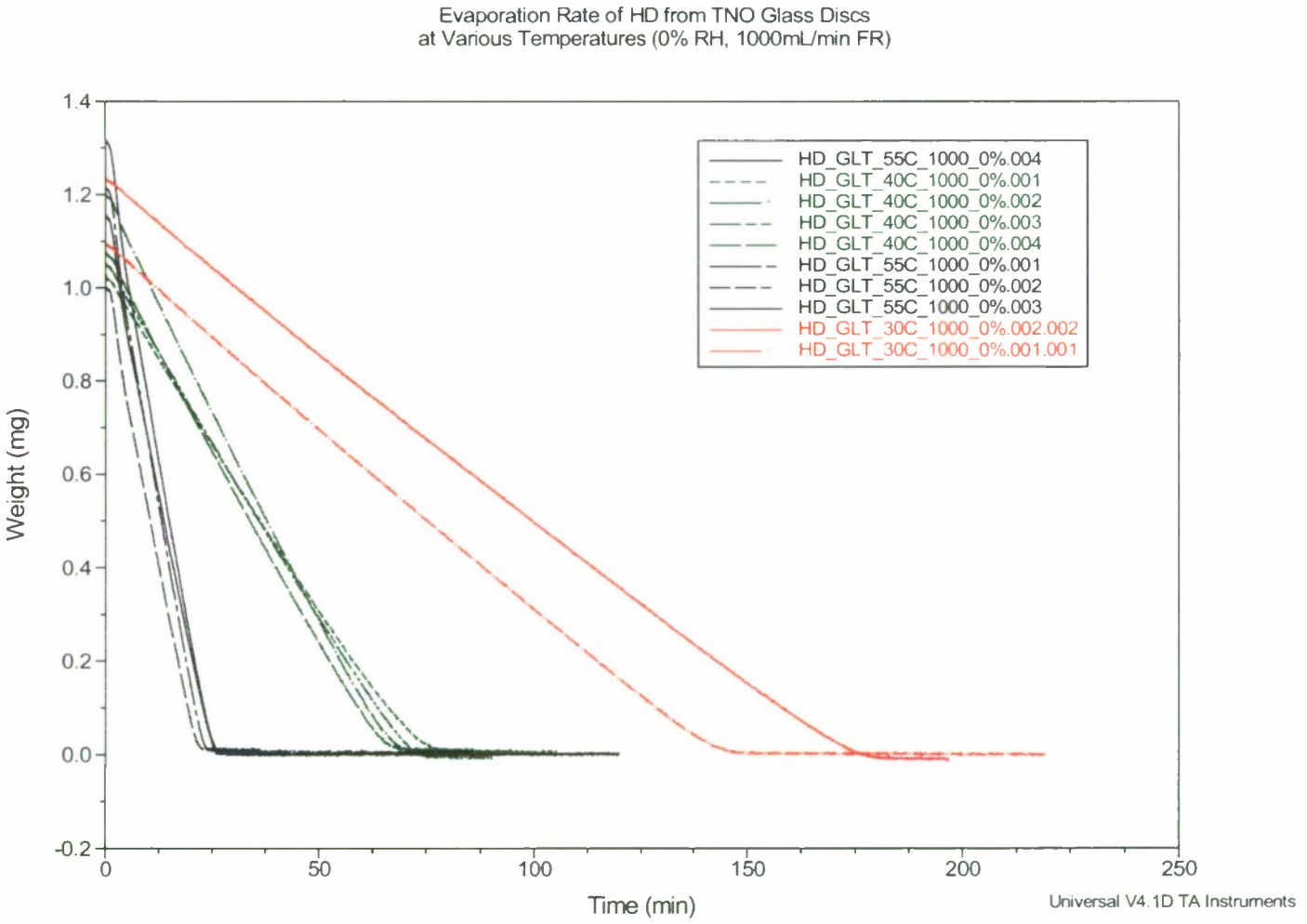

Figure 19. Comparison of HD Evaporation Rate from Glass (TNO) at Various Temperatures: 0% RH and 1000 mL/min Flow Rate.

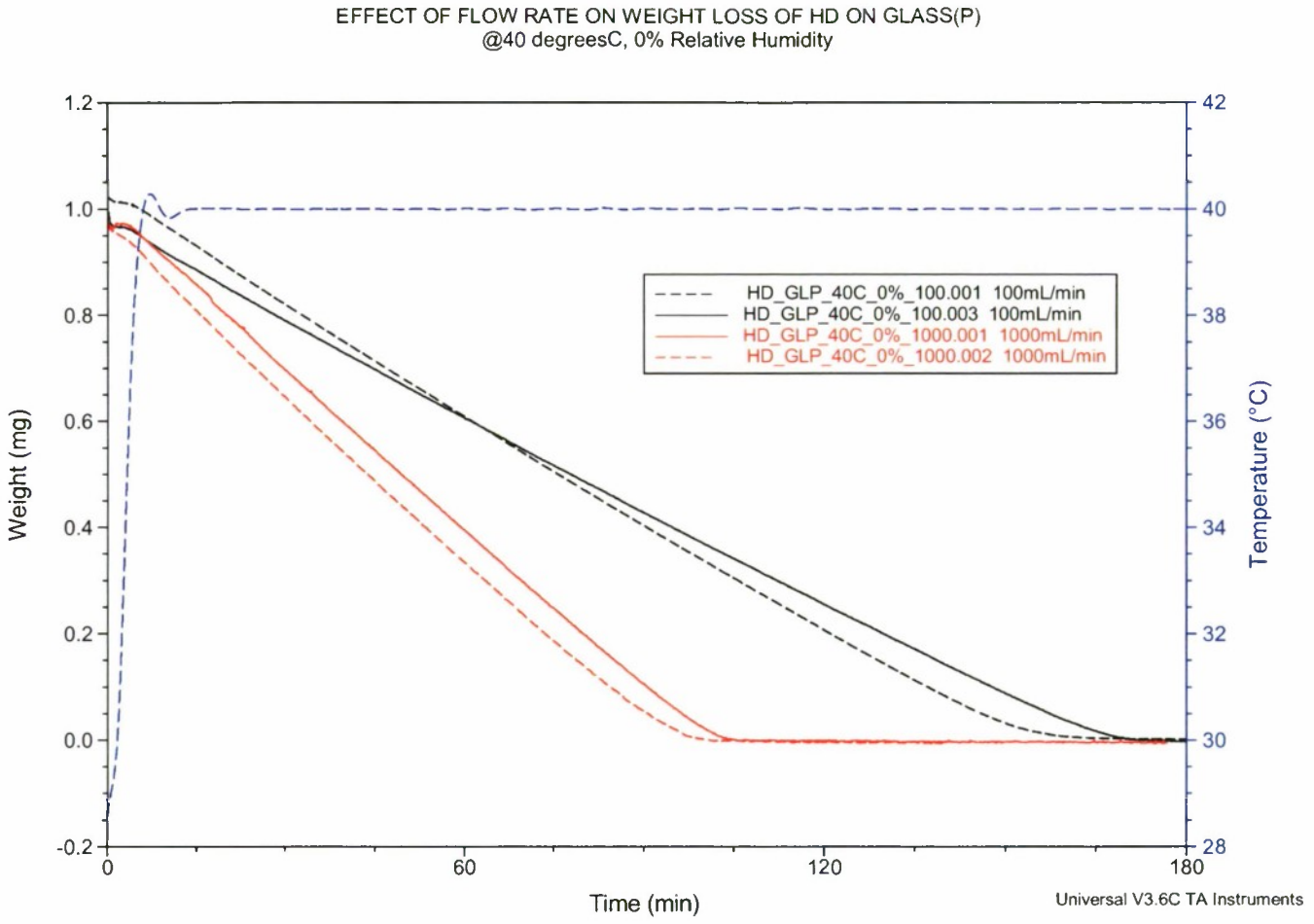

Figure 20. Comparison of HD Evaporation Rate from Glass (Window) at Various Flow Rates: @ 40 °C and 0% RH.

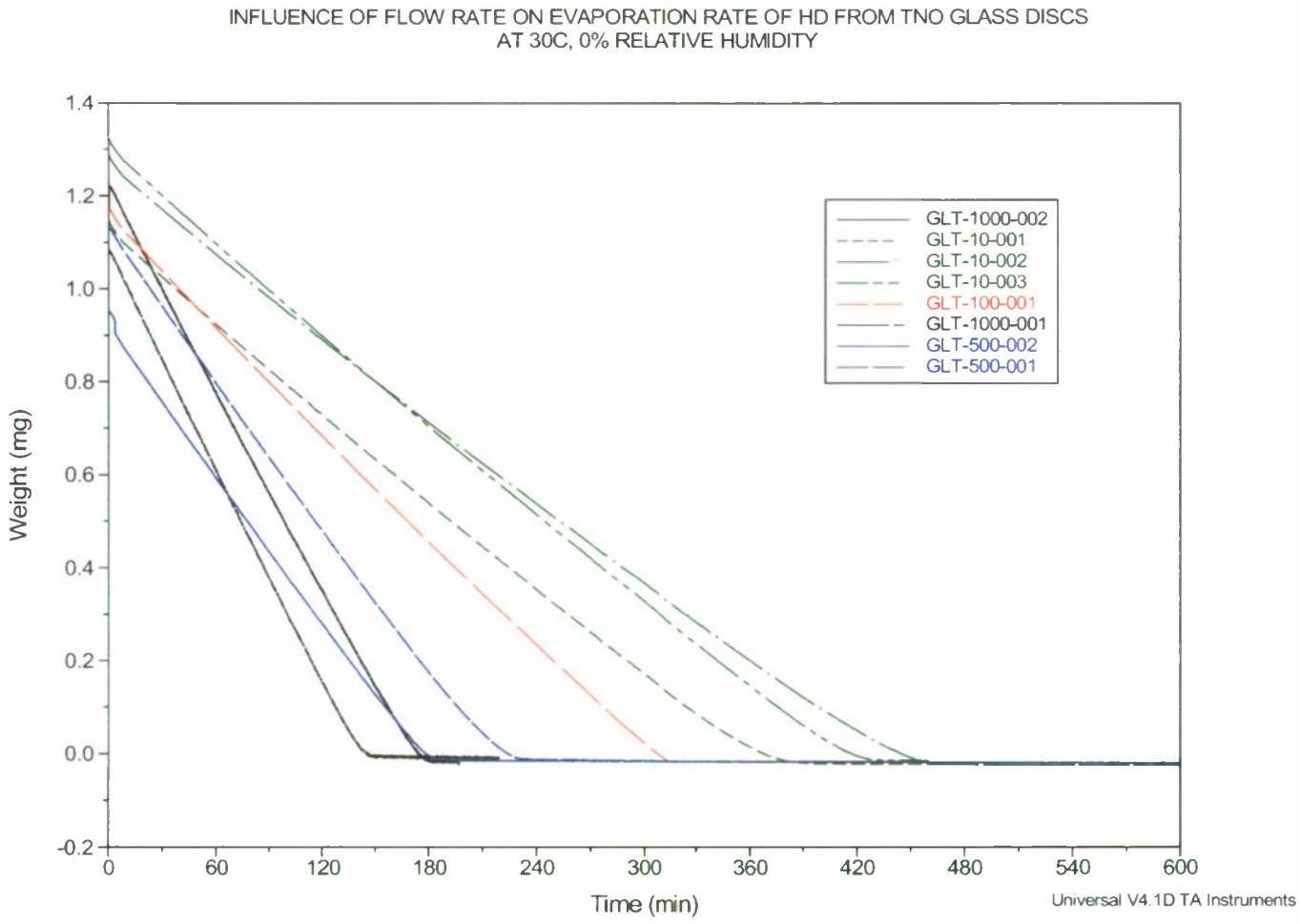

Figure 21. Comparison of HD Evaporation Rate from TNO Glass at Various Flow Rates: @ 30 °C and 0% RH.

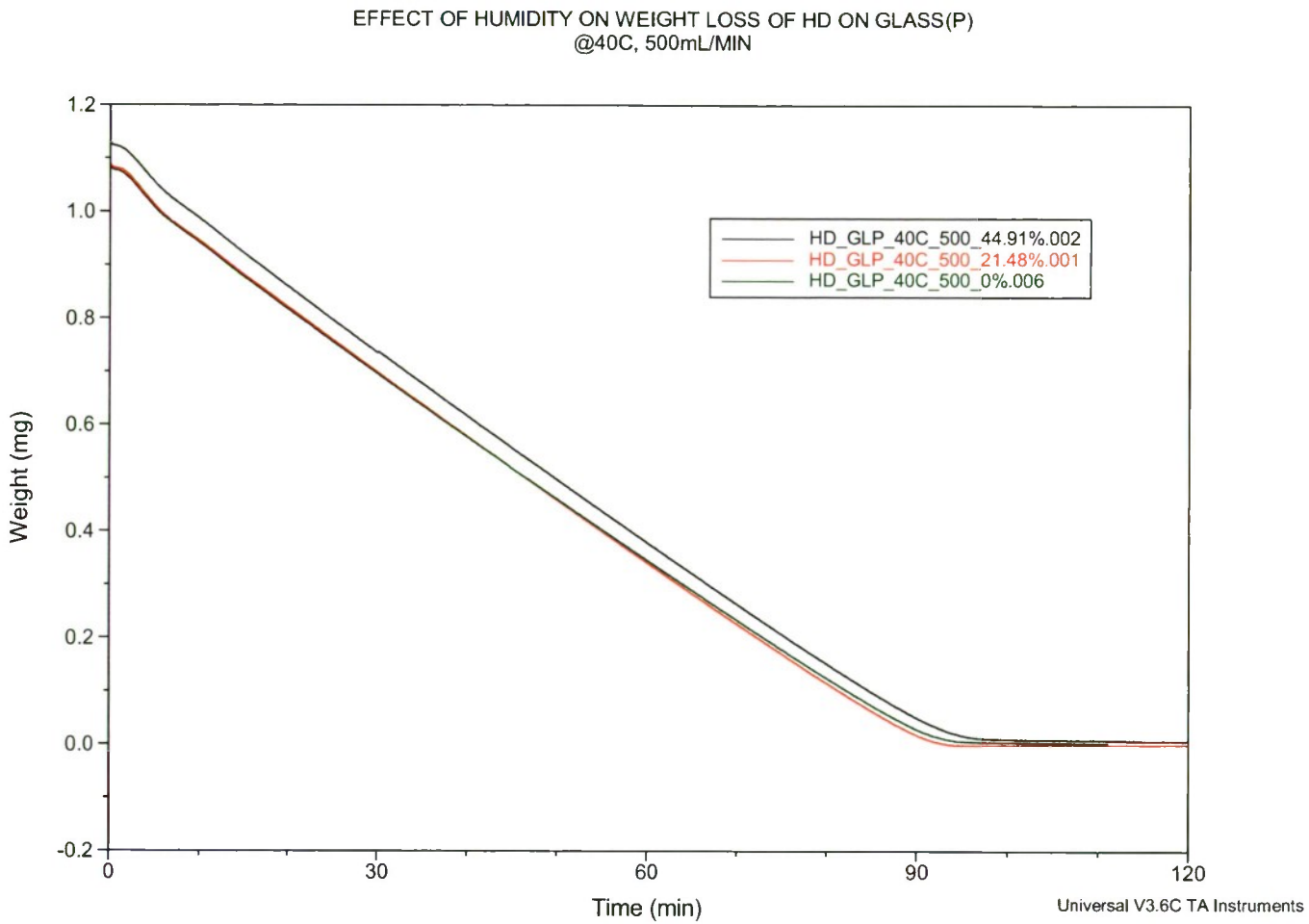

Figure 22. Comparison of HD Evaporation Rate from Glass (Window) at Various RHs: @ 40 °C and 500 mL/min Flow Rate.

3.3 HD on Teflon

The HD droplets on Teflon tend to bead up, probably due to the low surface energy of Teflon, resulting in a smaller surface area. This caused the drops to evaporate slowly from the Teflon surface (3.2 μg/min) compared to their evaporation from the glass (5.0 μg/min) or aluminum surfaces (7.7 μg/min) under the same environmental condition (shown in Figure 23). Actually, the HD drops spread out more on the aluminum surface than they did on the glass surface, thus evaporating faster than they did on the other two surfaces. Also, the evaporation rate is not as linear as in the case of glass or aluminum, which indicates that the surface area of the drop changed throughout the evaporation process. Figure 24 shows drop size effect on the evaporation of HD drops from a Teflon surface. As shown before, in the case of either glass or aluminum, increase in the drop size increased the evaporation rate of HD under the experimental condition. When the drop size was increased from 1 to 3.5 μL on glass, the evaporation rate increased from 2.746 μg/min to 4.403 μg/min (1.60x). Increasing the drop size to 6 μL resulted in an evaporation rate of 6.089 μg/min (2.22x), at 30 °C, with a flow rate of 100 mL/min. On Teflon, when the drop size was increased from 1 to 3.5 μL , the evaporation rate increased from 3.202 μg/min to 5.029 μg/min (1.57x). Increasing the drop size to 6 μL resulted in an evaporation rate of 7.336 μg/min (2.29x), at 30 °C, with a flow rate of 1000 mL/m. Figure 25 shows flow rate effect on the evaporation of HD drops from the Teflon surface. As expected, faster flow rate increased the evaporation rate of HD under the experimental condition. The results are summarized in Table 6.

4. CONCLUSIONS

The microbalance wind tunnels provide reproducible and useful measurements of an evaporation and desorption process describing the environmental fate of chemical contaminants. Weight loss of HD demonstrated near zero order rates for aluminum and glass, indicating film evaporation from droplets that spread over a large wetted area at low contact angle. The spreading rate and wetted area were greater for glass and aluminum than for Teflon; therefore, the rates were more rapid for glass and aluminum than for Teflon. The initial evaporation rates were often about the same rate for different drop sizes, showing parallel evaporation curves, with time to complete evaporation increasing smoothly with increased droplet size. Slight variations from this pattern can be attributed to the larger surface area for the bigger drop. Environmental factors (e.g., flow rate and temperature) influenced the HD evaporation rate as expected; but, relative humidity has apparently little, if any, effect on the HD evaporation rate on these surface materials.

Table 6. Evaporation Rates of HD Droplets from Teflon Surface Measured by Microbalance Wind Tunnel (TGA) at 30 °C and 0% RH.

Run No.	Evaporation Rate by TGA (µg/min)	Dropsize (µL)	Ave. Rate (µg/min)	Flow Rate (mL/min)	Instrument (Figure)
TEF1001	3.715	1.0	3.202 ± 0.370	1000	TGA2950 (24)
TEF1002	2.727				
TEF1003	3.131				
TEF1004	3.054				
TEF1005	3.382				
TEF3001	4.342	3.5	5.029 ± 0.782	1000	TGA2950 (24)
TEF3002	4.607				
TEF3003	6.150				
TEF3004	5.806				
TEF3005	4.978				
TEF3006	4.292				
TEF6003	8.395	6.0	7.336 ± 0.947		
TEF6004	7.042				
TEF6005	6.571				
TEF2010	2.332	1.0	2.284 ± 0.164	10	SDT Q600 (25)
TEF3010	2.067				
TEF4010	2.460				
TEF5010	2.275				
TEF1100	2.852		2.928 ± 0.180	100	
TEF2100	2.710				
TEF3100	3.060				
TEF4100	3.091				

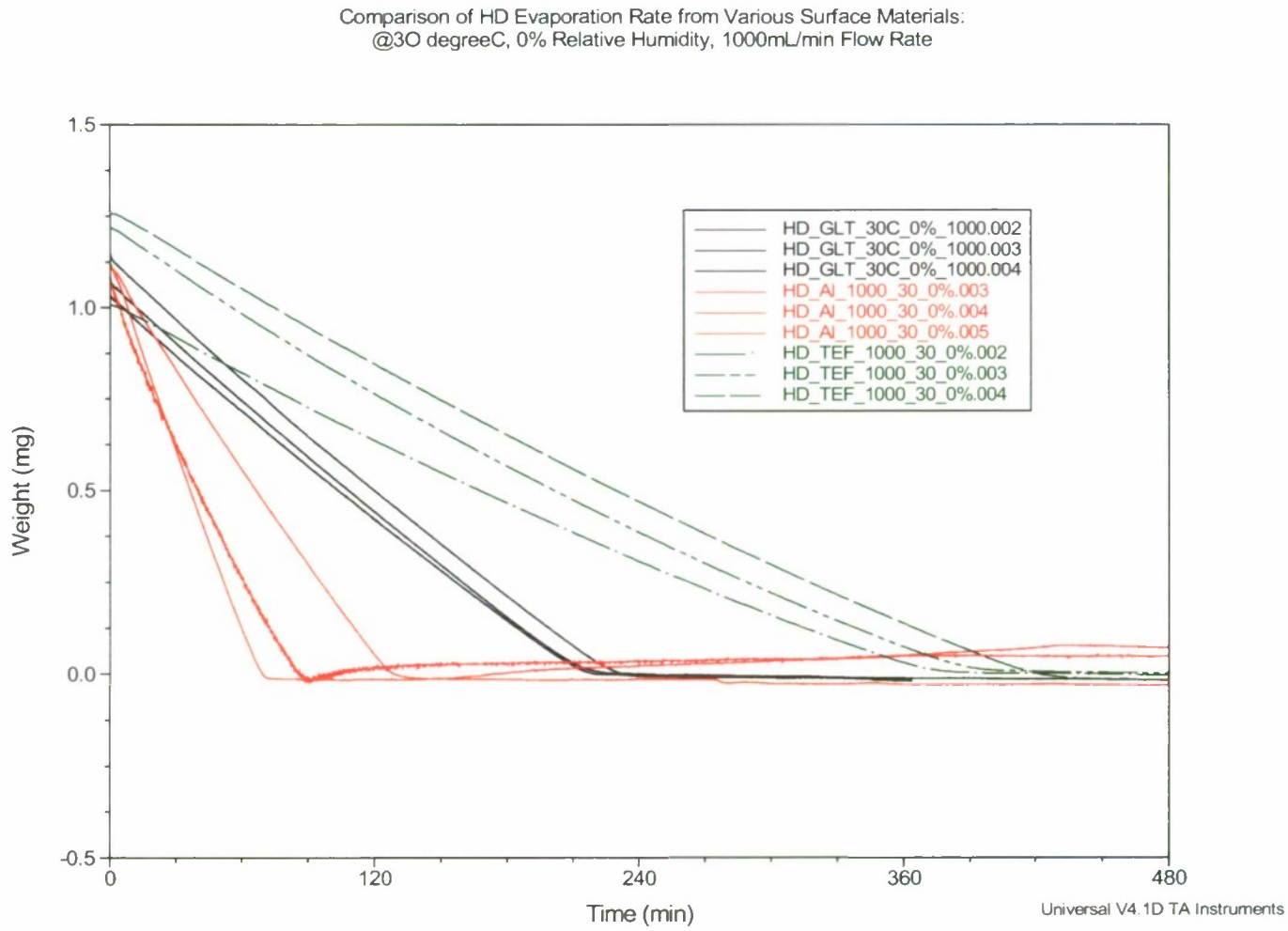

Figure 23. Comparison of HD Evaporation Rate from Various Surface Materials: @ 30 °C, 0% RH, and 1000 mL/min Flow Rate.

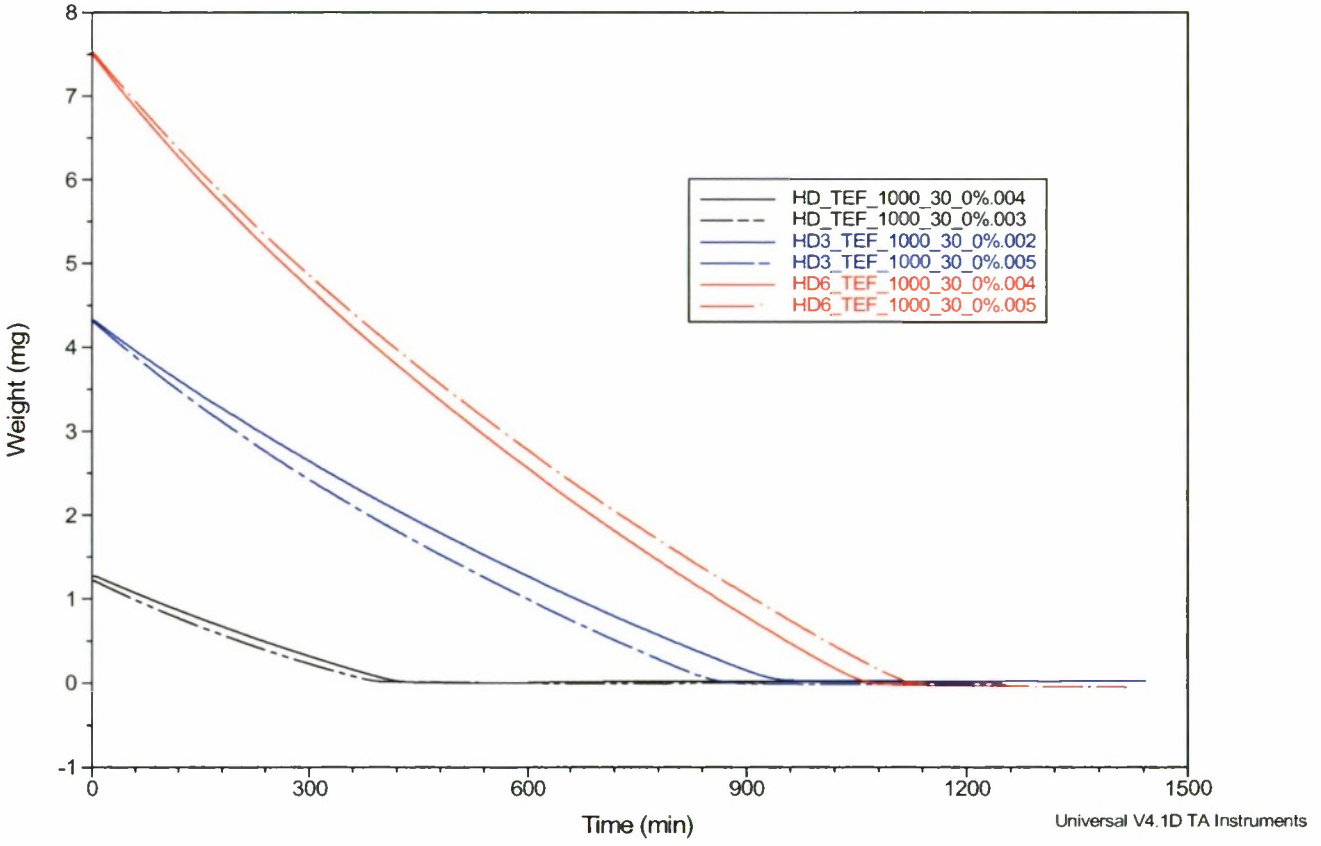

Figure 24. Comparison of HD Evaporation Rate from Teflon Discs: Drop Size Effect @ 30 °C, 0% RH, and 1000 mL/min Flow Rate.

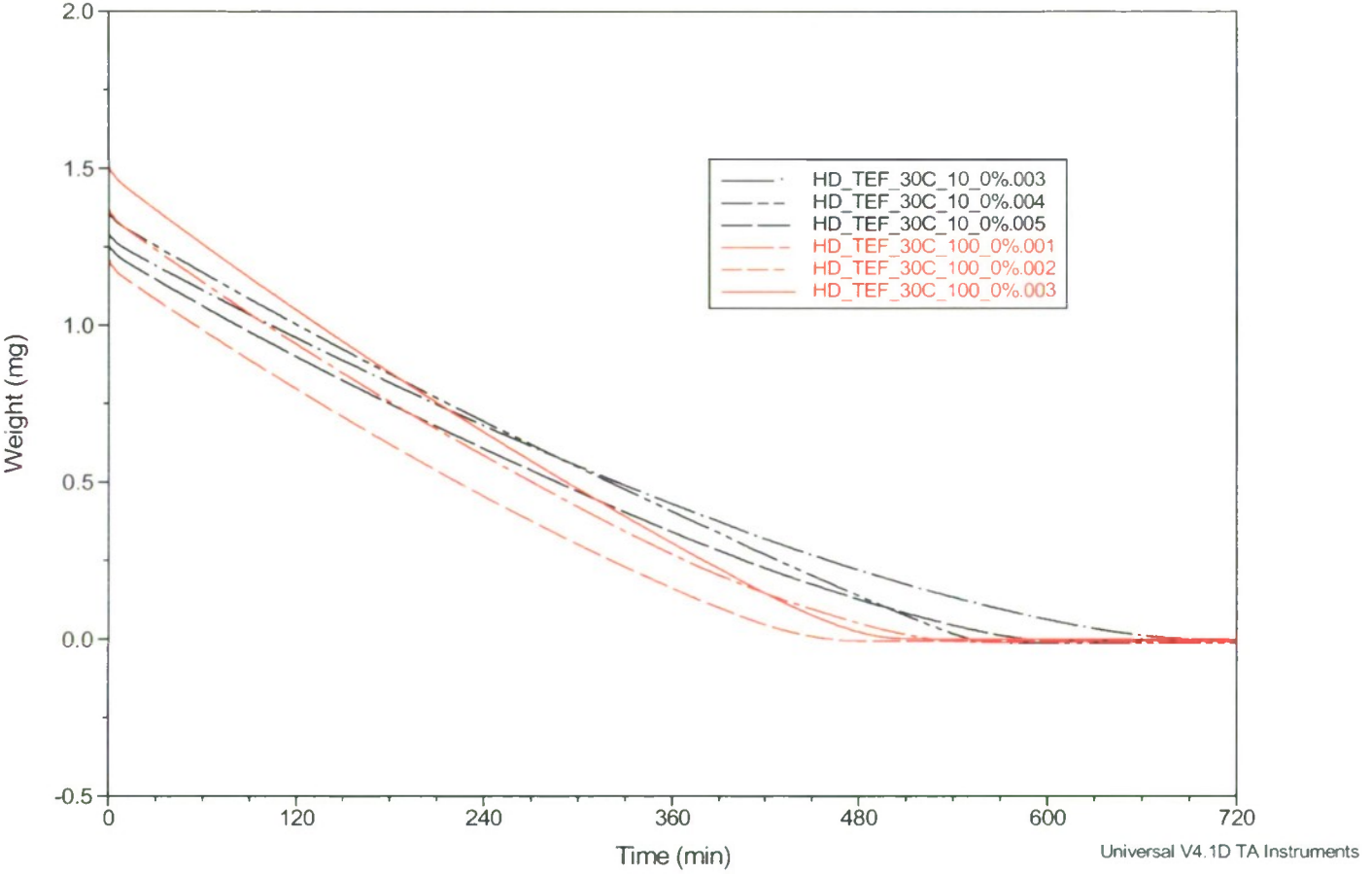

Figure 25. Comparison of HD Evaporation Rate from Teflon Discs: Flow Rate Effect @ 30 °C, 0% RH, and 1 µL Drops.

Blank

LITERATURE CITED

1. Bauer, T.J. *Software Design Description for the Chemical/Biological Agent Vapor, Liquid, and Solid Tracking (VLSTRACK) Computer Model, Version 3.0;* NSWCDD/TR-99/6; Naval Surface Warfare Center: Dahlgren, VA, 1998; UNCLASSIFIED Report (AD-B244 341).

2. Shuely, W.J.; McHugh, V.M.; Ince, B.S. *Development of Computer-Controlled Thermogravimetric Instrumentation for Measurement of Environmental and High Temperature Volatilization and Desorption of Contaminants from Polymeric Materials;* CRDEC-TR-88054; U.S. Army Chemical Research, Development and Engineering Center: Aberdeen Proving Ground, MD, 1988; UNCLASSIFIED Report (AD-A195 934).

3. Savage, J.J.; D'Onofrio, T.G.; Durst, H.D.; Kilpatrick, W. *Environmental Fate of Chemical Agents: Final Report for Defense Technology Objective CB.42*; ECBC-TR-532; U.S. Army Edgewood Chemical Biological Center: Aberdeen Proving Ground, MD, 2007; UNCLASSIFIED Report (AD-B333 475).

4. Weber, D.J.; Molnar, J.W.; Shuely, W.J. Environmental Fate of Toxic Chemicals on Surface Materials in Laboratory Wind Tunnels: Measured and Computed Wind Speeds and Flow Fields (AD-E502 039). In *Proceedings of the 2002 Joint Service Scientific Conference on Chemical and Biological Defense Research*, 19-21 November 2002; ECBC-SP-015; Berg, D.A., Compiler; U.S. Army Edgewood Chemical Biological Center: Aberdeen Proving Ground, MD, 2003; UNCLASSIFIED Report (AD-M001 523).

5. Shuely, W.J.; Nickol, R.G.; Pence, J.J.; Weber, D.J.; Molnar, J.W.; Hong, S.H.; Sumpter, K.B. Methodology Development for Measurement of Agent Fate in an Environmental Wind Tunnel (AD-A449 671). In *Proceedings of the 2003 Joint Service Scientific Conference on Chemical and Biological Defense Research*, 17-20 November 2003; ECBC-SP-018; Berg, D.A., Compiler; U.S. Army Edgewood Chemical Biological Center: Aberdeen Proving Ground, MD, 2005; UNCLASSIFIED Report (AD-M001 851).

6. Weber, D.J.; Molnar, J.W.; Scudder, M.K. Characterization of the Flow Field, Wind Speed Profiles, and Turbulence Intensity in Environmental Wind Tunnels for Measurement of Agent Fate (AD-A449 675). *In Proceedings of the 2003 Joint Service Scientific Conference on Chemical and Biological Defense Research*, 17-20 November 2003; ECBC-SP-018; Berg, D.A., Compiler; U.S. Army Edgewood Chemical Biological Center: Aberdeen Proving Ground, MD, 2005; UNCLASSIFIED Report (AD-M001 851).

7. Weber, D.J.; Molnar, J.W.; Scudder, M.K.; Shuely, W.J. Characterization of the Flow Field and Wind Speed Profiles in Microbalance Wind Tunnels for Measurement of Agent Fate (AD-A449 676). In *Proceedings of the 2003 Joint Service Scientific Conference on Chemical and Biological Defense Research*, 17-20 November 2003; ECBC-SP-018; Berg, D.A., Compiler; U.S. Army Edgewood Chemical Biological Center: Aberdeen Proving Ground, MD, 2005; UNCLASSIFIED Report (AD-M001 851).